FORMATION DAMAGE DUE TO IRON PRECIPITATION IN LIMESTONE, DOLOMITE AND SANDSTONE CORES

A Thesis

by

AYTEN KHALED MOHAMED ABDELHALIM RADY

Submitted to the Office of Graduate and Professional Studies of
Texas A&M University
in partial fulfillment of the requirements for the degree of

MASTER OF SCIENCE

Chair of Committee,	Hisham Nasr-El-Din
Committee Members,	Jerome Schubert
	Mahmoud El-Halwagi
Head of Department,	A. Daniel Hill

May 2016

Major Subject: Petroleum Engineering

ABSTRACT

Formation damage due to iron precipitation continues to be a major problem in the oil field. Research has established that as the pH of injected acid increases, iron (III) ions start to precipitate and block the pores in the formation, significantly reducing production. However, where exactly this iron precipitates and how iron precipitation changes with different lithologies has not yet been comprehensively studied.

Coreflood experiments were conducted on carobonate (calcite and dolomite) and sandstone cores to assess the effects of temperature and iron concentrations on the degree of damage caused by iron precipitation during an acid job. The temperature values tested were 200 and 300°F. Iron concentrations ranging from 5,000 to 10,000 ppm were used. The core effluent samples were analyzed by ICP (Inductively Coupled Plasma) to measure the concentrations of key cations.

Coreflood experiments, revealed that iron precipitates across the entire core. Iron precipitation was severely detrimental in sandstone cores compared to those composed of calcite and dolomite. While limestone cores showed the least formation damage from iron precipitation, coreflood tests indicated that as the iron concentration increases, the damage was more evident. On the other hand, increasing the temperature adversely affected sandstone and dolomite cores, but improved the final permeability of limestone cores.

In this study, the location of the iron precipitation is determined for three different lithologies. The effects of different parameters are studied to determine the best conditions

that would lead to a decrease in iron precipitation and hence prevent formation damage. Iron control agents are not always needed, as previously thought.

DEDICATION

I dedicate this work to my father who has always pushed me to study abroad, and to my mother and sister for their endless support.

ACKNOWLEDGEMENTS

I would like to express a special acknowledgment for my supervisor and mentor, Dr. Hisham Nasr-El-Din, who provided me with the opportunity to study here at Texas A&M University and to conduct research under his guidance and expertise. He has generously offered me continuous support and motivation.

I would also like to thank my committee members Dr. Jerome Schubert and Dr. Mahmoud El-Halwagi for their continuous motivation.

Finally I would like to thank Ms. Gia Alexander for all her efforts and time she spent in editing my work.

TABLE OF CONTENTS

Page

LIST OF FIGURES

Page

LIST OF TABLES

Page

CHAPTER I

INTRODUCTION AND LITERATURE REVIEW*

Well Stimulation

Acid well stimulation was first proposed in 1896 (Walker et al 1991). Acid injection into the formation was proposed to remove damage near the wellbore region and restore permeability to its original value. The acidizing operation is accomplished by injecting reactive fluids (commonly hydrochloric acid) below the fracturing pressure of the formation. The objective to an acid treatment if to dissolve and disperse the rock while creating highly conductive wormholes in order to increase the productivity of oil and gas wells (Ghommem et al. 2015). Carbonate reservoirs are mostly heterogeneous, which makes them have different a wide range of permeability. The dissolution mechanism in carbonate rocks involves channeling. The process of channeling occurs when the matrix material is dissolved away as a result of the reactive fluid injected. One common example is the dissolution of carbonate rock by the usage of reactive hydrochloric acid fluid. Channeling causes the creation of a random network of channels. The channels formed due to the dissolution process in carbonate rocks are non-uniform. This is mainly because not all parts of the rock interact with the acid solution (Hoefner and Fogler, 1988). The stimulation fluids injected during the acidizing process, choose to flow through the path

* Part of this chapter is reprinted with permission from "Iron Precipitation in Calcite, Dolomite and Sandstone cores" by Ayten Rady and Hisham Nasr-El-Din, 2015 SPE Russian Petroleum Technology Conference, 1-18, Copyright 2015 Society of Petroleum Engineers

of least resistance where the permeability is high and/or the damage (skin) is low (Nasr-El-Din et al 2008). As a result of this selective behavior of the acid, some parts of the formation may remain untouched by the acid. A number of models can be used to predict the distance to which the acid penetrates and the amount of rock that will be dissolved and removed by the acid.

The two dominant carbonate reservoirs present in the oil field are calcite and dolomite (Sayed et al 2013). It is generally assumed that the reaction of acid with limestone ($CaCO_3$) formations is much faster than the reaction of acid with dolomite $(CaMgCO_3)_2$ formation during well stimulation (Taylor et al 2006).

In solid-liquid reactions, the following sequence occurs (Lund et al 1973):

1. Diffusion of the liquid phase reactants to the immediate vicinity of solid-liquid interfaces
2. Reaction at the solid-liquid interface
3. Diffusion of the products away from the interface

The rate of the reaction will depend on the slowest step. If the slowest step is the “is the diffusion of reactants and products to and from the solid-liquid interface, then the reaction is mass-transfer-limited. If the slowest step is the surface reaction itself, then the reaction is surface-reaction-limited” (Taylor et al 2004).

Calcite Acidizing

Hydrochloric acid reacts with limestone as follows:

$$2HCl + CaCO_3 \rightarrow CaCl_2 + H_2O + 2CO_2 \quad \text{..... (I-1)}$$

The reaction between hydrochloric acid and calcite is a fast one. The overall rate of the reaction depends on the "detachment from the mineral surface (surface reaction effect) and diffusional transport of dissolved aqueous species from this surface through an interfacial layer into the bulk solution (transport effect)" (Alkattan et al 1998). Lund et al. 1975 studied the dissolution of calcite in hydrochloric acid using a rotating disk system. Results from his experiments concluded that the reaction between hydrogen ion adsorbed on the surface and the solid calcite is rate limiting. The study also showed that calcite reacts with 1 M HCl approximately 650 times faster than dolomite (Taylor et al 2004).

Dolomite Acidizing

Hydrochloric acid reacts with dolomite as follows:

$$4HCl + CaMg(CO_3)_2 \rightarrow CaCl_2 + MgCl_2 + 2H_2O + 2CO_2 \quad \text{..... (I-2)}$$

In this reaction, 4 mol of hydrochloric acid react with 1 mol of dolomite to form calcium and magnesium chloride, carbon dioxide and water. The hydrochloric acid/dolomite reaction is considered a heterogeneous reaction because it occurs between a solid and a liquid. The heterogeneous reaction takes place at the interface between the two phases (Anderson 1991).

Lund et al. 1973 conducted experiments using a rotating disk reactor to determine if the reaction between dolomite and hydrochloric acid is reaction limited or diffusion

limited or in between. They conducted a series of experiments using dolomite at temperatures of 25 to 100 °C, with an acid concentration ranging from 0.01 to 9.0 g mol/L and disk rotational speeds from 50 to 500 rev/min. “They found that the dissolution of dolomite is surface reaction limited at low temperatures (25 and 50 °C) and mass transfer limited at higher temperatures (100 °C)” (Sayed et al 2013).

Sandstone Acidizing

The main objective of acidizing a sandstone rock is to remove the formation damage that is caused by drilling, workover or completion processes. The goal is to restore the original permeability of the sandstone formation. During the acidizing process, continuous variations in the porosity and permeability of the formation occur as a result of the dissolution of the rock matrix and the precipitation of the reaction by-products. Three steps are needed when acidizing sandstone reservoirs: pre-flush, main flush and post-flush. Typically hydrochloric acid is used for the pre-flush treatment. The mixture of hydrochloric acid (HCl) and HF, known as mud acid, is used extensively as the main treatment. In sandstone reservoirs, HF can dissolve alumino-silicates and silica while the HCl keeps the pH low enough to prevent the reaction by-products from precipitating (Ji et al. 2015).

Typically, sandstone formations contain a certain percentage of indigenous clays as part of their mineral composition. These clays can be a part of the matrix, or exist as coating on the pore walls or even accumulating within the pores. Clay present in the sandstone formation can cause severe permeability reduction due to their tendency to plug

interconnecting pore throats. Incompatible fluid injection can cause clay swelling or fines migration which will lead to permeability reduction. The permeability of Grey Berea sandstone is mostly affected by clay particles migration since they contain little or no swelling clays (Musharova et al 2012). The clay content of the Grey Berea sandstone is mostly kaolinite and illite, which are migratory and/or dispersible clays that are sensitive to sudden changes in salinity, pH, flow rate and temperature (Khilar and Fogle 1983). Schembre and Kovscek (2004) show that fine clay particles are released from the pore walls when the equilibrium conditions are disturbed particularly due to high temperature, high pH and moderate aqueous phase salinity.

Experiments have shown that the permeability of the Berea sandstone core decreases rapidly and significantly when fresh water is injected into the pore space to displace the initial brine solution that was present. This colloidal phenomenon, known as water sensitivity, results mainly due to the release of the clay particles from the pore walls. The clay particles then start migrate and block the pore throats causing damage to the formation and a decrease in the initial permeability value (Kia et al 1987).

Sandstone clays are relatively more stable with acid fluids in the pore spaces as they will keep the walls negatively charged. Changing the solution acidity (pH) from acid to alkaline may cause the release of clay particles and hence pore throat blockage (Musharova et al 2012).

Mechanical fines migration can occur in sandstone reservoirs when the flowing fluid reaches a threshold velocity. If the velocity of the flowing fluid exceeds this threshold

velocity, the clay particles and fines can detach from the surface and mobilize (Hanafy et al. 2015).

Khilar and Fogle (1983) state that the temperature affects both the initiation and the rate of permeability reduction. As the temperature is lowered, the time at which the permeability begins to decrease is delayed. The rate of reduction in permeability was found to decrease with decreasing temperature. This conclusion has also been confirmed by Musharova et al (2012), indicating that experimental coreflood results show that the clay particle stability is affected by temperature and the higher the temperature the faster the migration process of the clays. As the temperature increases, the clay fines become sensitive and detach from the rock surface therefore causing pore bloackage. In the Grey Berea sandstone, the kaolinite disperses as discrete particles while the illite disperses by pore bridging.

Formation Damage

Hydrochloric acid (HCl) offers many advantages when stimulating wells that resulted in its widespread use (Walker et al. 1991). However, HCl has several disadvantages; iron precipitation due to hydrochloric acid stimulation is one of the serious problems encountered. Iron precipitation can result in plugging the flow channels and impairing the permeability near the wellbore, which will lead to a production decline. The acid solution can become contaminated with iron as a result of reacting with iron-containing products and equipments such as storage and mixing tanks, well casing, coiled tubing, pipes, fittings, and well tubulars (Taylor et al. 2001; Assem et al. 2013). In some other cases, the

formation itself may contain iron-minerals, such as hematite, magnetite, pyrite, siderite, and chlorite, or the formation brine may have significant amounts of iron in solution (Dill and Fredette 1983; McLeod 1984). Typically, the iron contained in siderite and chlorite is Fe(II), while hematite is Fe(III) (Crowe 1986).

Iron can be found in several oxidation states; +2, +3, and +6. The +6 state is rarely ever found. "The oxidation states of +2 and +3 correspond to ferrous and ferric ions, respectively. The oxidation state of iron depends on the oxidizing or reducing characteristics of its solvent medium and on the type of anion with which it is associated. In an oxidizing medium such as air, the ferric ion is more stable, whereas under reducing conditions or in an anaerobic medium, ferrous ion is more stable." The ratio of the Fe(II) to Fe(III) is an important parameter to be determined, on average it has been estimated that Fe(II) to Fe(III) ratio of spent acid is 5:1. This ratio varies greatly depending on well conditions and the type of formation being treated. Rust or scale formed by oxygen corrosion will largely be of the Fe(III) type, and this will be mostly found in water injection wells. Hence when dissolved by acid Fe(III) will present a potentially more serious precipitation problem. Producing wells, however, usually present less of a problem since most Fe scales formed in the pipe are of the Fe(II) type (Crowe 1985).

A study of formation water samples shows that from 57 to 2,075 mg/l of ferrous iron can be in solution (Dill and Smolarchuk 1988). The largest source of dissolved iron comes as a result of the reaction of acid with the casing. This is because of the large surface area of the casing (Taylor and Nasr-El- Din 1999). Gougler et al. (1985) initiated a field study to identify the magnitude of the iron problem; the study indicated that between 9,000

to 10,000 ppm of dissolved iron is injected into the formation during the acidizing process as corrosion products (Gougler et al. 1985). The magnitude of the problem increases at higher temperatures because the reaction rate of HCl becomes faster, and as a result, corrosion also increases. Corrosion inhibitors are often used to mitigate the corrosion impact; special additives such as corrosion intensifiers are required to compensate for loss of the inhibitors through degradation at temperatures above 300°F. The addition of corrosion intensifiers substantially increases the cost. The cost of intensifiers can exceed 5% of the treatment cost. Most of the available corrosion inhibitors and intensifiers are environmentally hazardous. Another drawback of corrosion inhibitors and intensifiers is that they may enter the formation, get adsorbed onto the reservoir rock, and subsequently change the wettability (Rabie and Nasr-El-Din 2015; Assem et al. 2013)

One important factor that minimizes ferric hydroxide precipitation is the reduction of Fe(III) by metallic Fe. A certain amount of the dissolved Fe(III) is reduced as the acid travels down the pipe as a result of the following reaction (Eq.I-3) (Crowe 1985).

$$2\ Fe^{+++} + Fe^{0} \rightarrow 3\ Fe^{++} \quad \text{(I-3)}$$

The usual cause of iron precipitation is the formation of insoluble gelatinous ferric hydroxide as the pH increases in spent acid. Typically Ferric hydroxide, $Fe(OH)_3$ is the most damaging iron precipitant following an acid treatment (Smith et al. 1969). Both iron (II) and iron (III) can precipitate, but iron (III) hydroxide precipitates first from spent acid since it comes out of solution and precipitates at a pH of 1 (Eq. I-4). Iron (II) hydroxide precipitates at pH values greater than 6, making it less of a problem when

acidizing sweet wells because spent acid reaches a pH of only 5.5 (Eq. I-5) (Taylor et al. 1999b; Crowe 1986).

$$Fe^{+3} + 3OH^{-} \leftrightarrow Fe(OH)_3 \cdot mH_2O\downarrow \quad \text{Above pH 1} \ldots\ldots\ldots\ldots\ldots\ldots\ldots\ldots\ldots\ldots \text{(I-4)}$$

$$Fe^{+2} + 2OH^{-} \leftrightarrow Fe(OH)_2 \cdot nH_2O\downarrow \quad \text{Above pH 6} \ldots\ldots\ldots\ldots\ldots\ldots\ldots\ldots\ldots\ldots \text{(I-5)}$$

In sour wells, the magnitude of the problem increases because in the presence of hydrogen sulfide (H_2S), ferrous iron can precipitate as iron (II) sulfide at pH values greater than 1.9 as shown in Eq. I-6 (Taylor et al. 1999).

$$Fe^{+2} + H_2S \leftrightarrow FeS\downarrow + 2H^{+} \quad \text{Above pH 1.9} \ldots\ldots\ldots\ldots\ldots\ldots\ldots\ldots\ldots\ldots\ldots\ldots \text{(I-6)}$$

Hydrogen sulfide is a strong reducing agent that can reduce the ferric iron to the ferrous iron state and precipitate elemental sulfur. Having sulfur in the formation is a serious issue because it is very difficult to remove as it is not soluble in acid as shown in Eq. I-7 (Crowe 1986; Taylor et al. 1999a).

$$2Fe^{+3} + H_2S \rightarrow 2Fe^{+2} + 2H^{+} + S\downarrow \ldots\ldots\ldots\ldots\ldots\ldots\ldots\ldots\ldots\ldots\ldots\ldots\ldots\ldots\ldots\ldots\ldots\ldots \text{(I-7)}$$

When acidizing sandstones, live acid returns often are observed following the treatment. However this should not be interpreted as no precipitation can occur. Much of the acid in the area around the wellbore does remain unspent; however a zone of totally spent acid will be formed at the leading edge of the reaction front. In this area potentially damaging iron(III) precipitation will occur. In addition, the acid at this leading edge usually contains a greater portion of dissolved Fe resulting from dissolution of scale in the pipe.

Iron compounds that precipitate during acidizing will cause formation damage as they will settle and plug the pore spaces and pore throats, and as result the permeability of

the reservoir will be significantly reduced. Formation damage from precipitated iron compounds can be difficult to remove and will add costs (Taylor et al. 2001; Garzon et al. 2007).

Research Objectives

Formation damage due to iron precipitation is a major problem in the oil field. In this research, experiments have been conducted to understand the effect of iron precipitation in three different lithologies; limestone, dolomite and sandstone. Coreflood experiments are conducted to determine the effects of temperature and iron concentration on the different lithologies. This research aims to find the conditions where iron control agents would not be needed.

CHAPTER II

EXPERIMENTAL METHODOLOGY

Materials

Three different types of cores were used in conducting the experiments: Indiana limestone, Silurian dolomite, and Grey Berea sandstone. X-ray diffraction analysis indicated that the rock mineralogy for Indiana limestone was more than 98 wt% calcite ($CaCO_3$) as shown in **Tables 1** and **2**. **Tables 3** shows the mineral composition of the Silurian dolomite was more than 99 wt% calcium magnesium carbonate ($CaMg(CO_3)_2$). The mineralogy composition of the Grey Berea sandstone core was obtained by combining the results from X-ray powder diffraction (XRD), scanning electron microscopy (SEM), and X-ray fluorescence (XRF). The results are presented in **Tables 4** and **5**. All cores were 1.5 in. diameter and 6 in. length, however their permeability was different. Concentrated hydrochloric acid solutions (35.64%) were obtained from Sigma Aldrich, as well as formic acid (96%) and the ferric chloride, which was used as a source of iron (III) in the acid solution. A corrosion inhibitor was used in preparing the acid solution. The brine used for the sandstone cores was 5 wt% potassium chloride. The deionized water used throughout the experiments was obtained from a purification water system with a resistivity of 18.2 MΩ.cm at room temperature.

Compound	Concentration (wt%)
Al_2O_3	0.232
$CaCO_3$	98.3
Cl	0.0457
Fe_2O_3	0.107
K_2O	0.109
MgO	0.574
SiO_2	0.368
SnO_2	0.0144
SO_3	0.213
SrO	0.0227

Table 1— XRF analysis of Indiana Limestone core, compound wt%

Element	Concentration (wt%)
Al	0.123
C	11.8
Ca	39.4
Cl	0.0457
Fe	0.0751
K	0.0906
Mg	0.346
O	47.9
S	0.0853
Si	0.172
Sn	0.0113
Sr	0.0192

Table 2— XRF analysis for Indiana Limestone core, element wt%

Element	Concentration (wt%)
Ca	24.99
Mg	15.15
O	59.86

Table 3— XRF analysis for Silurian Dolomite core, element wt%

Compound	Concentration (wt%)
Albite	3
Calcite	2
Illite	2
Kaolinite	6
Quartz	87

Table 4— XRF analysis of Grey Berea Sandstone core, compound wt%

Element	Concentration (wt%)
Al	4.5
Ba	0.0347
Ca	0.327
Ce	0.0171
Cl	0.231
Fe	1.06
K	1.65
La	0.0384
Mg	0.651
Mn	0.0213
Na	0.502
O	50.9
S	0.0144
Si	39.5
Sn	0.0125
Ti	0.327
Zr	0.0552

Table 5— XRF analysis of Grey Berea Sandstone core, element wt%

Equipment

The coreflood setup used is shown in **Fig. 1** (Assem, 2013). Coreflood experiments were conducted to simulate the matrix acidizing treatment. Pressure and temperature were applied to mimic the reservoir conditions. The overburden pressure applied was around 1850-1900 psi, and a back pressure of 1100 psi was applied to ensure that there was a single phase flow and that the CO_2 was kept in solution at all times. Heating jackets were used to surround the core, and heating tapes were used to surround the flow lines to make sure that the system was at the desired temperature. Pressure transducers were connected to a computer, and the monitor screen was used to record the pressure drop across the core at all times. A Teledyne ISCO D500 syringe pump, was used to inject exact volumes of deionized water, brine, and acid into the core. Core effluent samples were collected and diluted to measure key cation concentrations (calcium, magnesium, and iron).

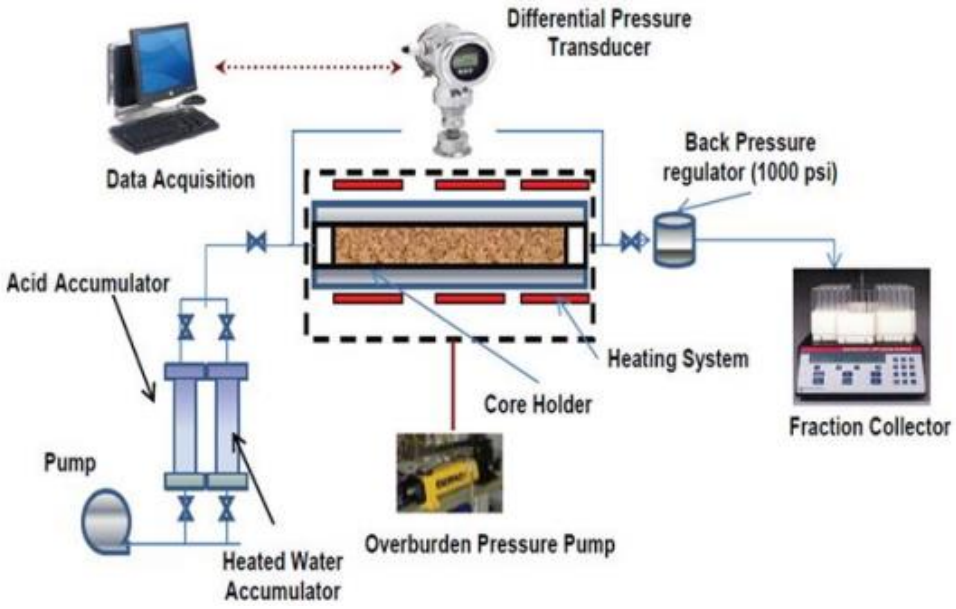

Fig. 1— Coreflood set-up.

The core effluent samples were diluted and analyzed using the Inductively Coupled Plasma Optical Emission Spectrometry (ICP-OES). A schematic of the ICP-OES is shown in **Fig. 2** (Assem, 2013). The concentration of the key cations were measure in each sample. For the case of the limestone and sandstone cores; the concentration of the calcium and iron were determined. While for the dolomite cores the concentration of calcium, magnesium and iron were measured. "Optical emission spectroscopy (OES) uses quantitative measurement of the optical emission from excited atoms to determine analyte concentration. Analyte atoms in solution are aspired into the excitation region where they are desolvated, vaporized, and atomized by a plasma. Electrons can be in their ground state or enter one of the upper level orbitals when energy is applied to them. A photon of light is emitted when an electron falls from its excited state to its ground state. Each

element has a unique set of wave length that it can emit". **Fig. 3** demonstrates the theory behind the ICP-OES (Assem 2013).

Fig. 2— ICP-OES set-up.

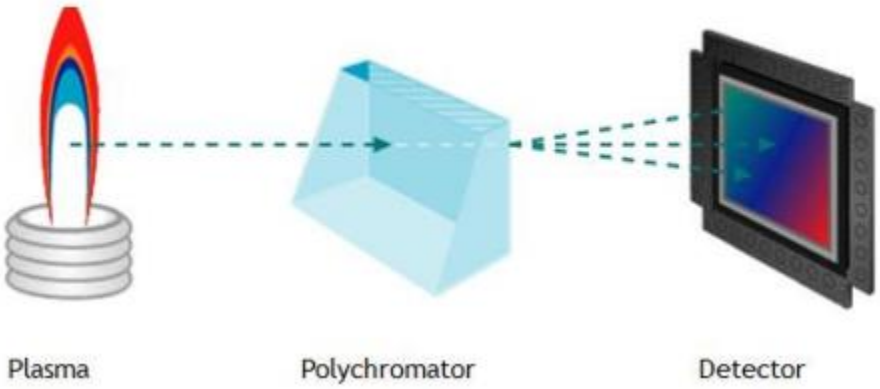

Fig. 3— ICP-OES theory.

Core Preparation

1. The first step in preparing the core is to dry it, by leaving it in the oven over night at 350°F. This step is important to get the dry weight of the core which will be used in calculating the pore volume.
2. The core is then saturated with de-ionized water for the case of limestone and dolomite cores and with 5wt% KCl brine for the sandstone cores. The core is saturated by submersing it in the water or brine for 4 hours while applying vacuum to suck all the air from the core and fill it with the desired fluid.
3. Once the core is saturated, the saturated weight and the dry weight will then be used calculate the pore volume using the following equation:

$$V_p = \frac{W_{wet} - W_{dry}}{\rho} \quad \text{..... (II-1)}$$

where:

V_p: Pore volume; cm^3

W_{wet}: Weight of saturated core; g

W_{dry}: Weight of dry core; g

ρ: Density of fluid used to saturate the core; g/cm^3

Acid Preparation

Several acid solutions were prepared for the different experiment conditions as described below:

Acid Solution 1: This solution consisted of 5 wt% hydrochloric acid and 1 vol% corrosion inhibitor. To prepare 100g of this solution the following amounts were used:

- Weight of HCl required using a 36.5 wt% concentration bottle = $\frac{5}{36.5} * 100 = 13.7g$
- 1 ml of corrosion inhibitor was added to the solution
- De-ionized water was added to the solution till its totoal weight was 100 g
- The solution was stirred using a magnetic stirrer for 30 minutes

Acid Solution 2: This solution consisted of 5 wt% hydrochloric acid, 1 vol% corrosion inhibitor and 10,000 ppm iron (Fe^{+3}). To prepare 100g of this solution the following amounts were used:

- Weight of HCl required using a 36.5 wt% concentration bottle = $\frac{5}{36.5} * 100 = 13.7g$
- 1 ml of corrosion inhibitor was added to the solution
- The iron was obtained from ferric chloride. The weight of ferric chloride added to the solution = $\frac{162.2*1}{56*100} * 100 = 2.896\ g$
- De-ionized water was added to the solution till its total weight was 100g
- The solution was stirred using a magnetic stirrer for 30 minutes

Acid Solution 3: This solution consisted of 5 wt% hydrochloric acid, 1 vol% corrosion inhibitor and 5,000 ppm iron (Fe^{+3}). To prepare 100g of this solution the following amounts were used:

- Weight of HCl required using a 36.5 wt% concentration bottle = $\frac{5}{36.5} * 100 = 13.7g$

- 1 ml of corrosion inhibitor was added to the solution
- The iron was obtained from ferric chloride. The weight of ferric chloride added to the solution = $\frac{162.2*1}{56*100} * 100 = 2.896\ g$
- De-ionized water was added to the solution till its total weight was 100g
- The solution was stirred using a magnetic stirrer for 30 minutes

Acid Solution 4: This solution consisted of 5 wt% hydrochloric acid, 2 wt% formic acid, 2 vol% corrosion inhibitor and 10,000 ppm iron (Fe^{+3}). To prepare 100g of this solution the following amounts were used:

- Weight of HCl required using a 36.5 wt% concentration bottle = $\frac{5}{36.5} * 100 = 13.7g$
- Weight of CH_2O_2 required using a 96.5 wt% concentration bottle = $\frac{2}{96.5} * 100 = 2.07g$
- 2 ml of corrosion inhibitor was added to the solution
- The iron was obtained from ferric chloride. The weight of ferric chloride added to the solution = $\frac{162.2*1}{56*100} * 100 = 2.896\ g$
- De-ionized water was added to the solution till its total weight was 100g

The solution was stirred using a magnetic stirrer for 30 minutes

Coreflood Experiment

1. The first step in the coreflood experiment is to measure the initial permeability of the core. This is done by injecting de-ionized water into the limestone and dolomite cores and injecting brine (5 wt% KCl) into the sandstone cores. The fluid is injected at a constant flowrate at room temperature and the pressure is recorded once it stabilizes. Using Darcy's equation for laminar flow the initial permeability of the core can then be calculated.
2. Once the initial permeability is measured, pressure and temperature are applied to mimic the reservoir conditions. The overburden pressure applied was around 1850-1900 psi, and a back pressure of 1100 psi was applied to ensure that there was a single phase flow and that the CO_2 was kept in solution at all times. The desired temperature was also applied and left for 90 minutes to ensure that the entire system has reached the necessary temperature and the pressure stabilized. The flow rate used to conduct all my experiments is 2 cm^3/min.
3. Once the system reaches the required temperature, only half pore volume of the acid solution is injected at a flow rate of 2 cm^3/min to prevent breakthrough of the core. Once the acid injection starts, samples are collected at the outlet to be analyzed using ICP-OES.
4. De-ionized water or brine is then injected into the core until the pressure is stable. The core effluent samples are collected at the outlet for analysis.
5. Once the pressure stabilizes, the core and the system is left to cool down back to room temperature and the final permeability is measured.

6. Throughout the entire coreflood experiment the pressure drop across the core was plotted versus time using the LABVIEW™ software.

ICP-OES Experiment

The samples that are collected from the coreflood experiment are diluted with de-ioninzed water and analyzed to measure the concentration of the key cations (calcium, magnesium and iron). The samples containing a reddish precipitant (iron) are diluted first by hydrochloric acid then de-ionized water. The acid is used to make sure that the iron is completely dissolved and doesn't block the lines of the ICP-OES system. The percent of iron recovered was then calculated from the initial amount of iron injected and the volume and concentration of each sample.

CHAPTER III

RESULTS AND DISCUSSION*

Four sets of experiments were conducted on each of the lithologies (calcite, dolomite and sandstone). The first set of tests involved the injection of 5 wt% hydrochloric acid without any iron at 200 °F to determine the effect of acidizing on the core permeability. The second set of experiments involved the injection of 5 wt% HCl and 10,000 ppm Fe (III) at 200 °F. The same conditions were repeated but at a higher temperature (300 °F) to study the effect of temperature on the final permeability. The last set of experiments involved the injection of 5 wt% HCl and 5,000 ppm Fe (III) at 200 °F.

Experimental Conditions 1

The first set of tests involved the injection of 5 wt% hydrochloric acid and 1 vol% corrosion inhibitor at 200 °F and flowrate of 2 cm^3/min. In this set of experiments no iron is injected to examine the effect of the acid on the different lithologies. **Table 6** summarizes the experimental results:

* Part of this chapter is reprinted with permission from "Iron Precipitation in Calcite, Dolomite and Sandstone cores" by Ayten Rady and Hisham Nasr-El-Din, 2015 SPE Russian Petroleum Technology Conference, 1-18, Copyright 2015 Society of Petroleum Engineers

Lithology	Iron Recovered (mg)	Initial Permeability (md)	Final Permeability (m)	Percent Change in Permeability
Limestone	0	155.33	192.25	23.76% Increase
Dolomite	0	29.76	32.93	10.65% Increase
Sandstone	171.6	102.55	97.13	5 % Decrease

Table 6— Results of the coreflood experiment using 5 wt% HCl, 1 vol% corrosion inhibitor at 200 °F and 2 cm^3/min

In the case of Indiana limestone, the initial permeability was 155 md and the final permeability was 192 md. The permeability of the limestone core increased by 23%. **Fig. 4** shows the pressure drop plotted against the time curve across the limestone core. The pressure has dropped slightly after the injection of the acid, indicating that acid reacted with the calcium carbonate and more channels have been created, hence the increase in the permeability. As mentioned earlier in the previous section, the permeability of the core is calculated from Darcy's equation. The relationship between pressure drop and permeability is inversely proportional, meaning that when the pressure drop decreases the permeability increases and vice versa. The increase in the core permeability was expected because of the reaction between the acid and the calcium carbonate. Similar results were published by Assem et al (2013); that study also showed that the permeability of the

Indiana limestone core increased after using 5-10 wt% HCl. **Fig. 5** shows the inlet of the core after the injection of the acid. The figure shows a wormhole created as a result of the acid injection into the core. The study by Assem et al (2013) also has pictures of the core inlet showing the formation of wormholes indicating that the results from the two studies match. The core effluent samples from the coreflood were analyzed using ICP, **Fig. 6** shows the concentration of the calcium and iron in the effluent samples. Fig. 6 shows that no iron was produced in the effluent samples, and this is expected as no iron was injected in the system. The initial concentration of the calcium is 0 mg/l then it starts to increase until it reaches a peak of 7304 mg/l. Then it drops again. This behavior is expected as initially the samples collected are mostly DI water being displaced by the injected acid. As the acid is injected into the formation, it starts to react with the $CaCO_3$, and calcium ions are produced as the by product. The gradual drop in the concentration of the calcium ions is due to the dissociation of the hydrochloric acid. The pH of the effluent samples have also been measured **Fig. 7**. Initially the pH of the samples is high (7.6), but as the acid starts to displace the water, the pH starts to drop until it reaches a minimum value of 5.3. As the acid starts to dissociate, the pH starts to increase again. The pH measurements of all the samples collected are greater than 1. The iron remains dissolved in the solution as long as the pH is less than 1; once the pH starts to increase, the solubility of Fe(III) decreases and it starts to precipitate in the formation causing damage (Taylor et al 1999b).

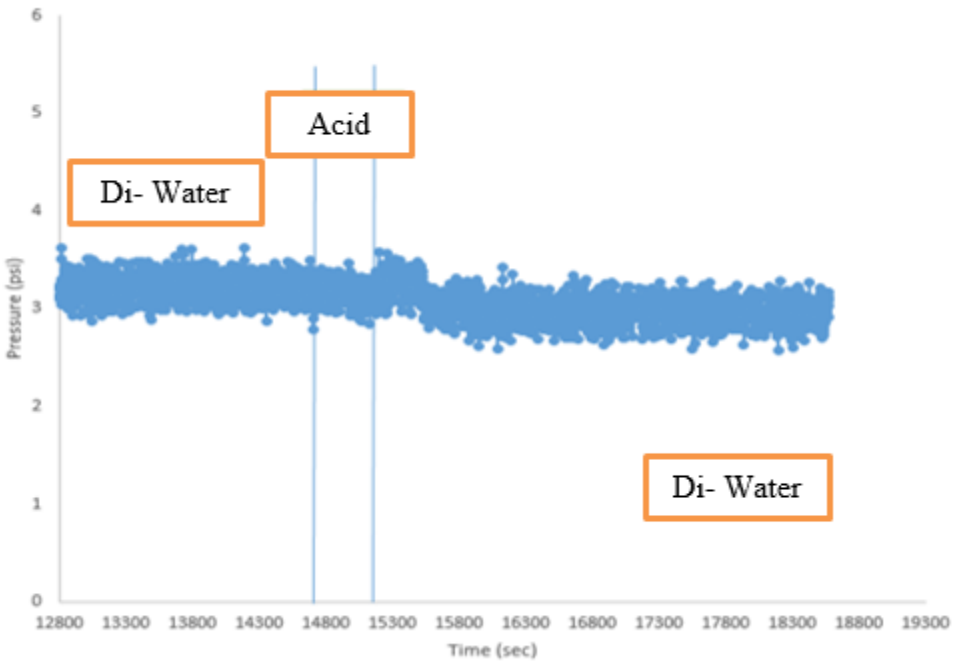

Fig. 4— Pressure profile across limestone core, 5 wt% HCl and 1 vol% corrosion inhibitor at 200 °F and 2 cm^3/min.

Fig. 5— Limestone core inlet after acidizing, 5 wt% HCl and 1 vol% corrosion inhibitor at 200 °F and 2 cm^3/min.

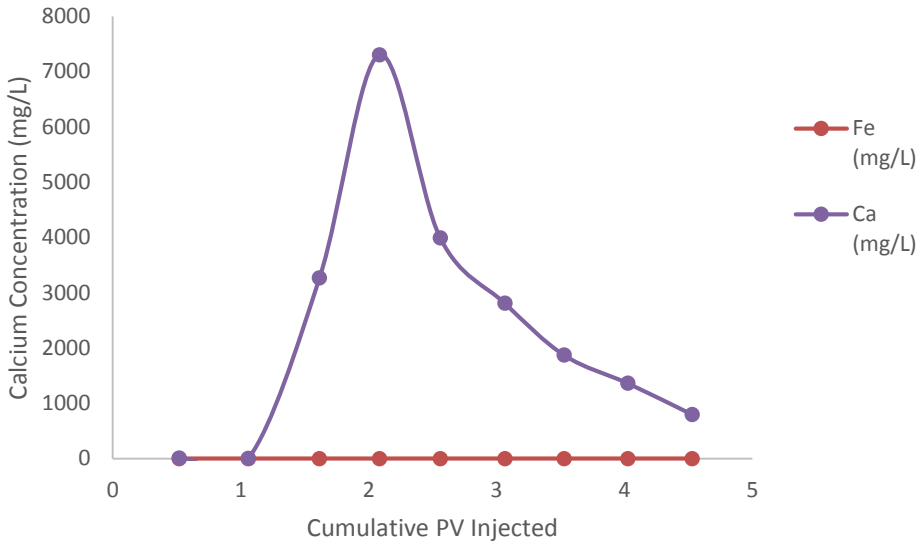

Fig. 6— Concentration of calcium and iron from limestone core, 5 wt% HCl and 1 vol% corrosion inhibitor at 200 °F and 2 cm^3/min.

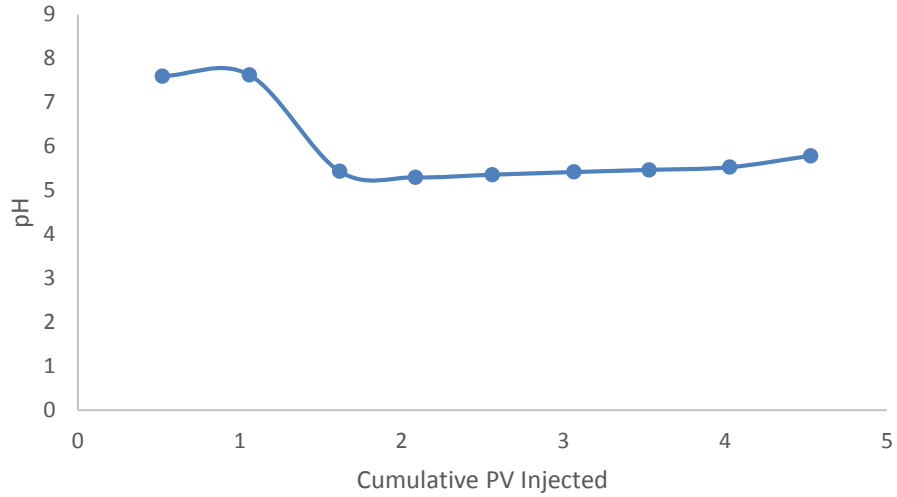

Fig. 7— pH from limestone core, 5 wt% HCl and 1 vol% corrosion inhibitor at 200 °F and 2 cm^3/min.

In the case of Silurian dolomite, the initial permeability of the core was 29 md and the final permeability was 33 md. After acidizing there was a 10% increase in the permeability. This behavior was expected as a result of the reaction between the hydrochloric acid and the $CaMg(CO_3)_2$. **Fig. 8** shows the pressure drop plotted against time curve across the dolomite core. Following the acid injection, the pressure drop increased slightly for a short period of time, then it decreased and stabilized at a final pressure less than the original pressure. This slight increase in the pressure drop can be explained as a result of the increase in the viscosity of the injected fluid. The final pressure drop is less than the original pressure drop, indicating an enhancement in the permeability. The percentage increase in the permeability of the dolomite core is less than that of the limestone core due to the strong bond between the magnesium and oxygen. **Fig. 9** shows the inlet of the dolomite core after the injection of the acid. The figure shows multiple small holes created as a result of the acid trying to create a path through the core. The core effluent samples from the coreflood were analyzed using ICP, **Fig. 10** shows the concentration of the calcium, magnesium and iron in the effluent samples. Fig. 10 further shows that no iron was produced in the effluent samples, and this is expected as no iron was injected in the system. The calcium and magnesium ions have the same trend; they both initially have a concentration of 0 mg/l and then reach a peak of 3,732 mg/l and 6,937 mg/l consecutively, then they gradually start to decrease. This is the same behavior that was observed in the Indiana limestone core, indicating that initially the collected sample is just DI water being displaced by the acid injected. The injected acid then reacts with the $CaMg(CO_3)_2$ to produce calcium and magnesium ions as byproducts. The gradual drop in

the concentration of the calcium and magnesium ions is due to the dissociation of the hydrochloric acid. The pH of the effluent samples has also been measured **Fig. 11**. Initially the pH of the samples is high (7.4), as the acid starts to displace the water the pH starts to drop until it reaches a minimum value of 5.0. As the acid starts to dissociate, the pH starts to increase again. Once again the pH measurements of all the samples collected are greater than 1, which means that the conditions necessary for Fe(III) to precipitate exists. This experiment shows that 5 wt% HCl is enough to enhance the permeability of the dolomite core by 11%.

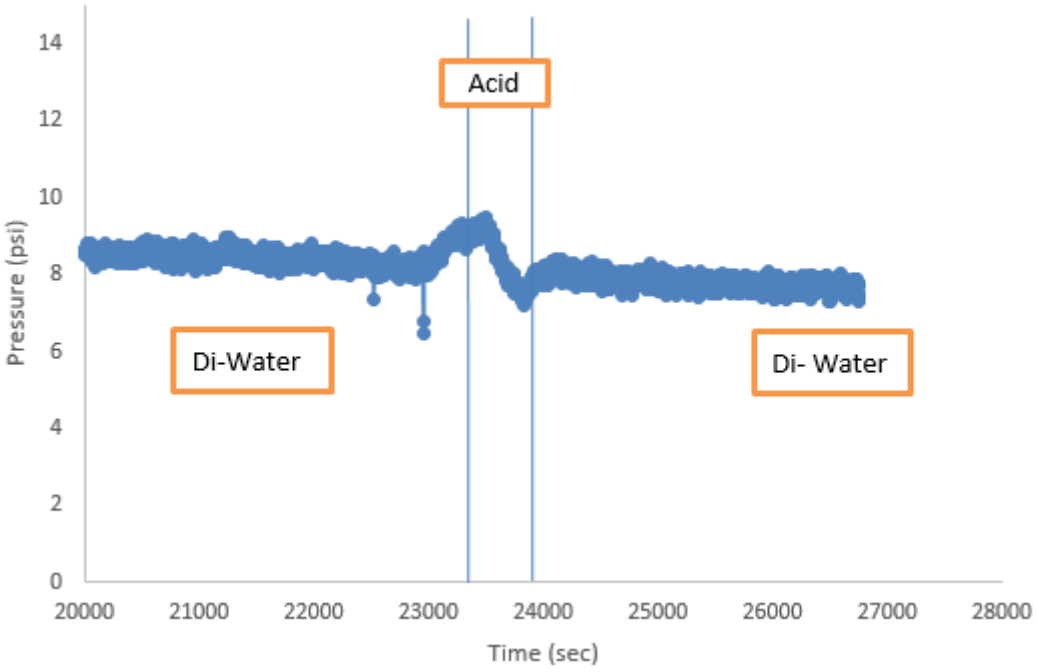

Fig. 8— Pressure profile across core dolomite core, 5 wt% HCl and 1 vol% corrosion inhibitor at 200 °F and 2 cm^3/min.

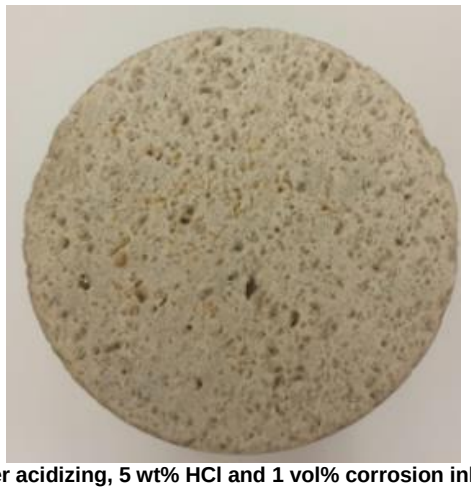

Fig. 9— Dolomite core inlet after acidizing, 5 wt% HCl and 1 vol% corrosion inhibitor at 200 °F and 2 cm^3/min.

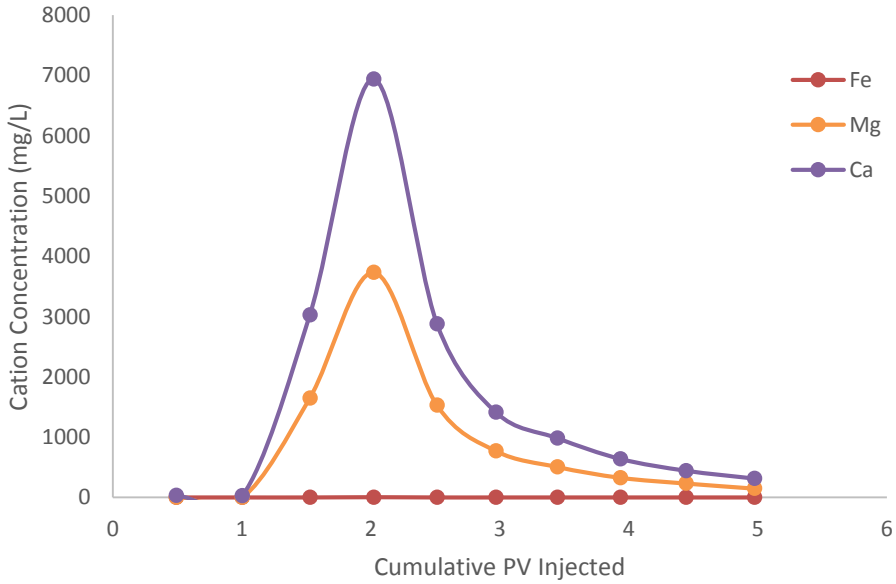

Fig. 10— Concentration of calcium, magnesium and iron from dolomite core, 5 wt% HCl and 1 vol% corrosion inhibitor at 200 °F and 2 cm^3/min.

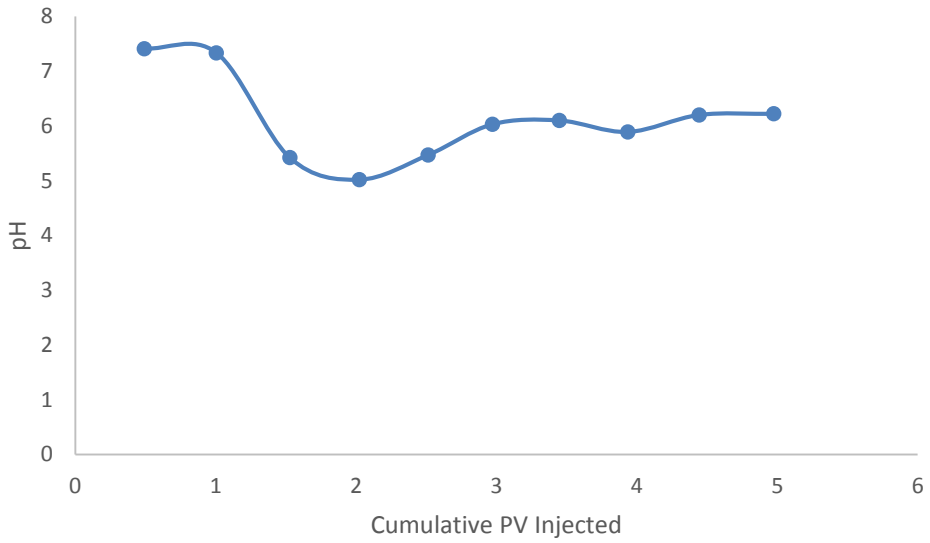

Fig. 11— pH from dolomite core, 5 wt% HCl and 1 vol% corrosion inhibitor at 200 °F and 2 cm^3/min.

In the case of the Grey Berea sandstone, the initial permeability of the core was 103 md, and the final permeability was 97 md. After acidizing there was a 5% decrease in the permeability. **Fig. 12** shows the pressure drop plotted against time across the sandstone core. The pressure drop is relatively constant during the entire experiment. This behavior is expected because the Grey Berea cores have approximately 2 wt% calcite is their mineral composition. **Fig. 13** shows the inlet of the core after the injection of the acid. Unlike the other two cases, there are no holes in the inlet of the core. Contrary to carbonates, the purpose of acidizing sandstone formations is to remove the damage; wormholes and channels are not created in the acidizing process. The core effluent samples from the coreflood were analyzed using ICP, **Fig. 14** shows the concentration of the calcium and iron in the effluent samples. The behavior of the concentration of calcium

followed the same trend as the limestone and dolomite formations; initially the concentration of the calcium is 0 mg/l then it starts to increase until it reaches a peak of 7,300 mg/l and then it drops again. However, iron was also found in the effluent samples, even though it was not injected into the system. Iron was produced gradually from the samples reaching a maximum value of 8,830 mg/l, then it dropped. Following the ICP results, XRF was used to identify the elements in the Grey Berea core. Iron was found to compose 1.06 wt% of the composition of the core. The pH of the effluent samples has also been measured **Fig. 15**. Initially, the pH of the samples is high (7.9). As the acid starts to displace the water the pH starts to drop until it reaches a minimum value of 2.25. As the acid starts to dissociate, the pH starts to increase again. Once again the pH values have exceed 1, which means that the conditions for iron precipitation are prevailing. For sandstone formations, the problem becomes more complicated because of the clay content. Clay particles are controlled by their mineralogy. The clay mineralogy can control factors such the shape and size and charge distribution of the clay. However the physiochemical "properties of the fluid such as ionic strength, pH, and temperature, together with clay mineralogy, determine the coagulation - dispersion processes, and, consequently, the rate of clay particle release." As a result, the pH of the system is of utmost importance when it comes to sandstone formation (Tchistiakov 2000). Musharova et al. (2012) studied the effect of pH on Grey Berea sandstone cores and found that in acidic solutions the edges of the clay minerals become positively charged, which causes the clay particles to migrate and plug the pore throats. This means that the damage caused in the sandstone core is

partly due to the iron precipitation and partly due to the clay particles plugging the pore throats.

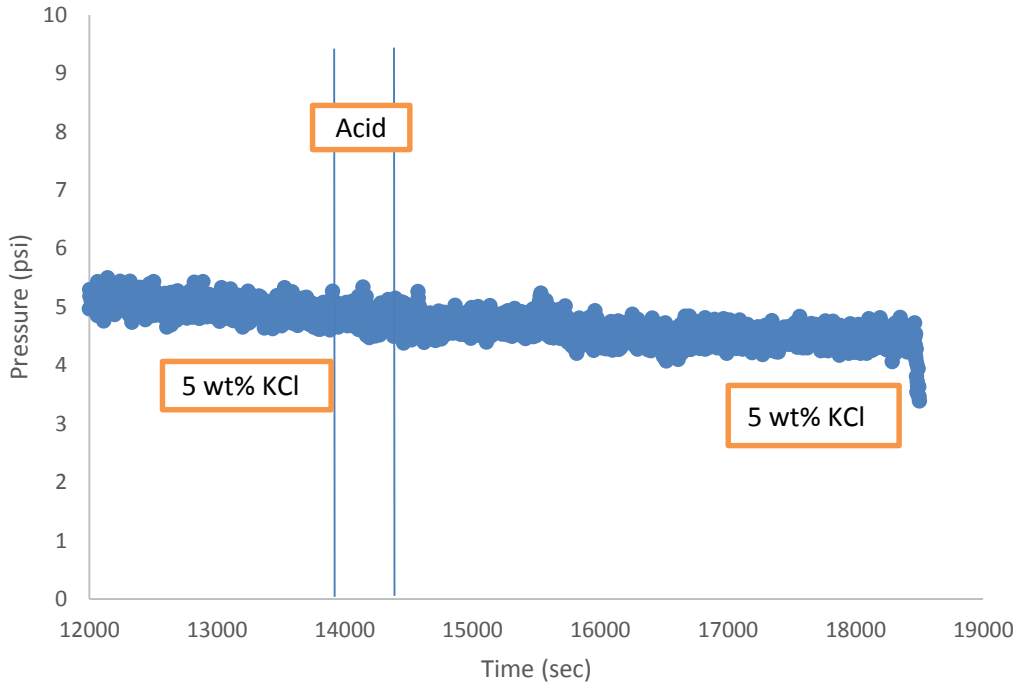

Fig. 12— Pressure profile across the sandstone core, 5 wt% HCl and 1 vol% corrosion inhibitor at 200 °F and 2 cm^3/min.

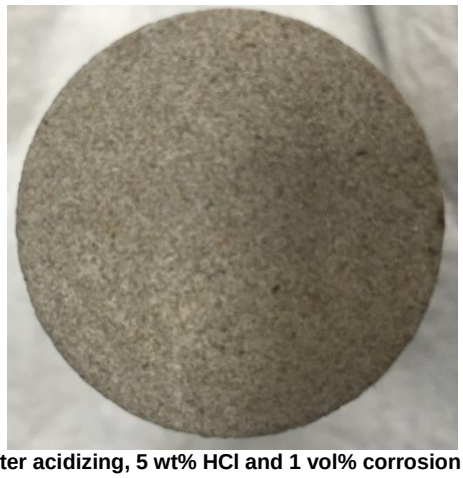

Fig. 13— Sandstone core inlet after acidizing, 5 wt% HCl and 1 vol% corrosion inhibitor at 200 °F and 2cm^3/min.

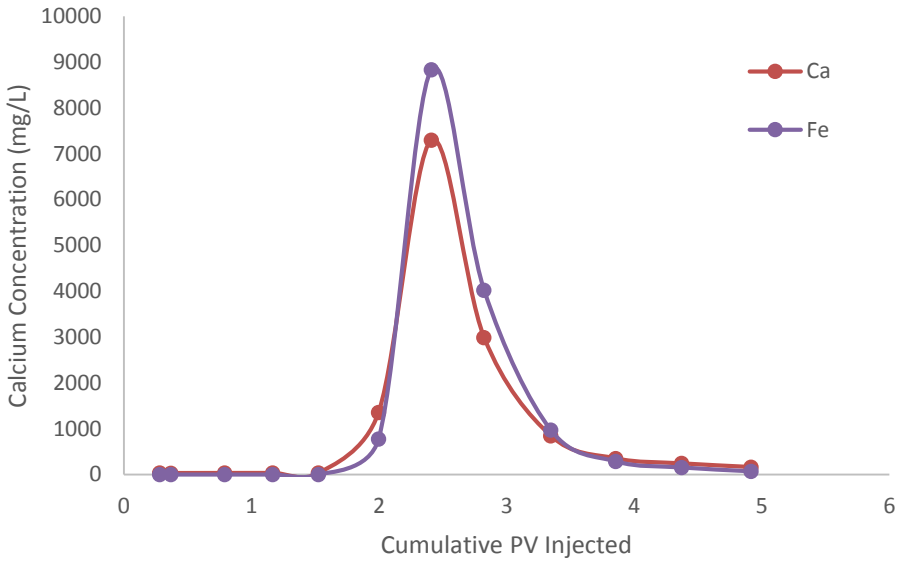

Fig. 14— Concentration of calcium and iron from sandstone core, 5 wt% HCl 1vol% corrosion inhibitor at 200 °F and 2 cm^3/min.

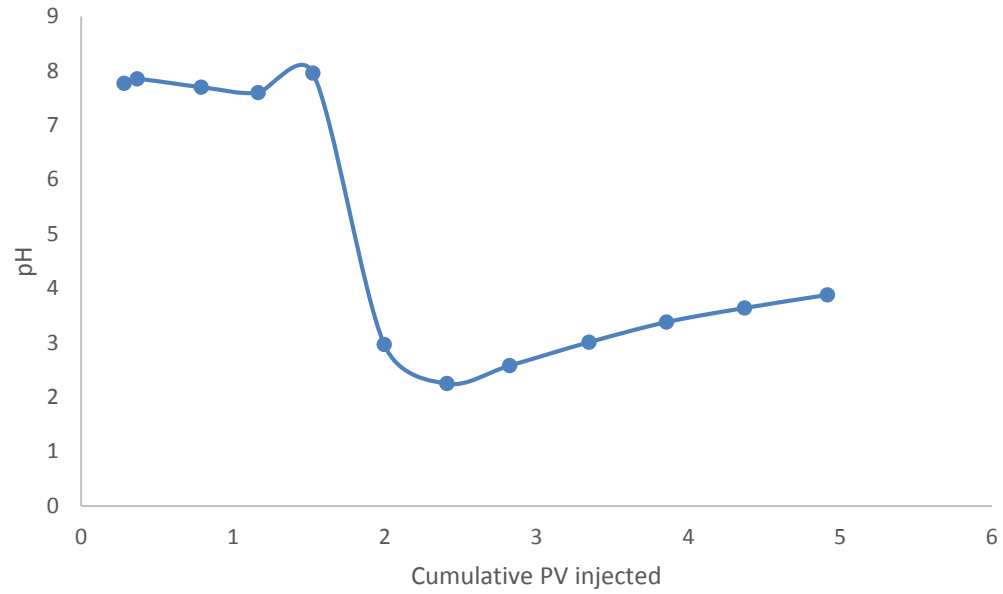

Fig. 15— pH from sandstone core, 5 wt% HCl and 1 vol% corrosion inhibitor at 200 °F and 2 cm^3/min

Experimental Conditions 2

The second set of experiments involves the injection of 5 wt% hydrochloric acid, 1 vol% corrosion inhibitor and 10,000 ppm of Fe(III) at 200 °F and a flowrate of 2 cm^3/min. In this set of experiments, the iron is injected to examine the effect of formation damage due to iron precipitation on the three different lithologies. **Table 7** (Rady and Nasr-El-Din, 2015) summarizes the results from the experiments conducted.

Lithology	Iron Recovered (%)	Initial Permeability (md)	Final Permeability (md)	Percent Change in Permeability
Limestone	41.3	149	139.4	6.7% Decrease
Dolomite	55.5	121.8	103.1	15.4% Decrease
Sandstone	135	164	139.6	17% Decrease

Table 7— Results of the coreflood experiment using 5 wt% HCl, 1 vol% corrosion inhibitor and 10,000 ppm Fe(III) at 200 °F and 2cm^3/min (Rady and Nasr-El-Din, 2015).

In the case of Indiana limestone, the initial permeability was 149 md and the final permeability was 139 md. The permeability of the limestone core decreased by 6%. This decrease was expected because of the iron injected into the formation. **Fig. 16** shows the pressure drop plotted against time across the limestone core. The pressure dropped slightly after the injection of the acid, indicating that it started to react with the calcium carbonate, and more channels have been created. However, the pressure then started to increase again. This increase in pressure occurred because the acid started to become spent and its pH started to rise causing the iron to precipitate and block the pores and channels and, hence damage the formation.

A recent study by Assem et al. (2013) acidized an Indiana limestone core using the same conditions, but obtained slightly different results. This study found no change in the

permeability after acidizing with 5 wt% HCl and 10,000 ppm of iron. The difference in the results of the two studies is minor and could be as a result of minor difference in preparing the acid solution or the coreflood set up used. **Fig. 17** shows the inlet of the core after the injection of the acid and iron. The figure further shows a wormhole created as a result of the acid injection into the core. The reddish color is due to the iron precipitation in the core. Assem et al. shows a similar picture of the core inlet showing the same reddish color and multiple wormholes. This again shows that the difference in the percentage of permeability change is minor and within experimental error.

The core effluent samples from the coreflood were analyzed using ICP, **Fig. 18** shows the concentration of the calcium and iron in the effluent samples. Fig. 18 further shows that iron was produced in the effluent samples; this is expected as 128.2 mg of iron was injected in the system. The initial concentration of the iron produced back into the samples is 0, but then it starts to increase until it reaches a peak of 1,833 mg/l then the concentration starts to drop back again. The total iron recovered was 53 mg which was 41% of the original iron injected. The percentage of the iron recovered in this experiment are much higher compared to the study by Assem et al. which only recovered 16% of the injected iron.

The concentration of the calcium ions also behaves in a similar fashion. The initial concentration of the calcium is 0 mg/l but then it starts to increase until it reaches a peak of 5,202 mg/l but then it drops again. This behavior is expected as initially the samples collected are mostly DI water being displaced by the injected acid. As the acid is injected into the formation, it starts to react with the $CaCO_3$ and calcium ions are produced as the

byproduct. The gradual drop in the concentration of the calcium ions is due to the dissociation of the hydrochloric acid. The pH of the effluent samples was not measured as they were diluted by hydrochloric acid to ensure that the iron precipitant is completely dissolved before the ICP-OES tests were run. However, in carbonate reservoirs the pH of spent acid is typically between 3 to 5. A study by Taylor et al. (1999b) measured the solubility of 10,000 mg/kg Fe(III) in calcium carbonate with 15 wt% HCl at room temperature. The study showed that once the pH of the solution rises above 1, the concentration of Fe(III) in the solutions starts to decrease. At a pH of 2 precipitation of Fe(III) is essentially complete (Taylor el al 1999b).

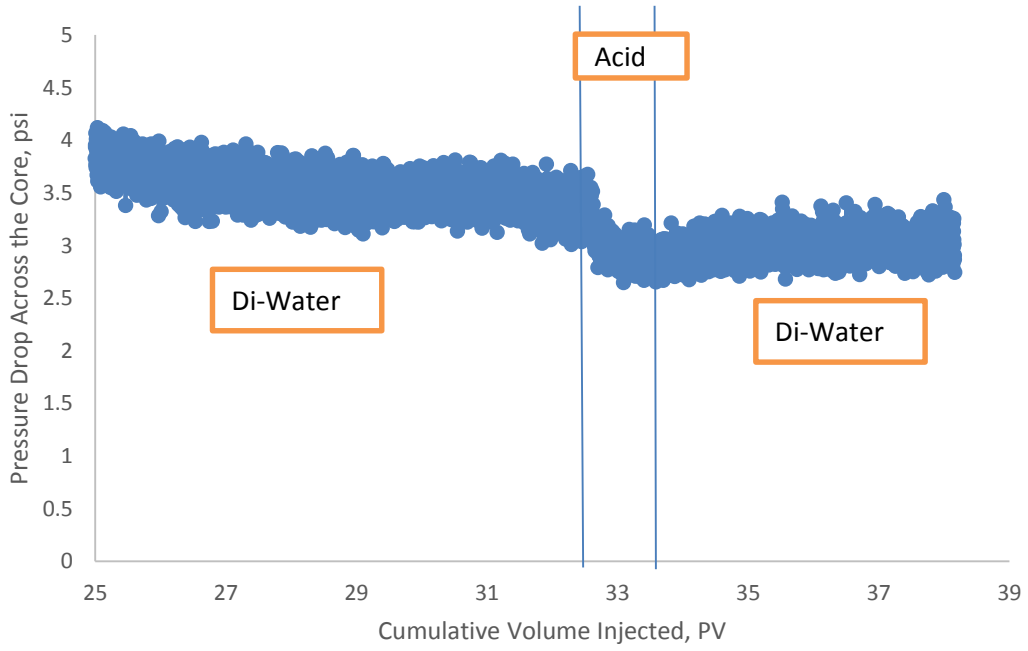

Fig. 16— Pressure profile across core limestone core, 5 wt% HCl, 1 vol% corrosion inhibitor and 10,000 ppm Fe(III) at 200 °F and 2cm^3/min (Rady and Nasr-El-Din, 2015).

Fig. 17— Limestone core inlet after acidizing, 5 wt% HCl, 1 vol% corrosion inhibitor and 10,000 ppm Fe(III) at 200 °F and 2 cm^3/min (Rady and Nasr-El-Din, 2015).

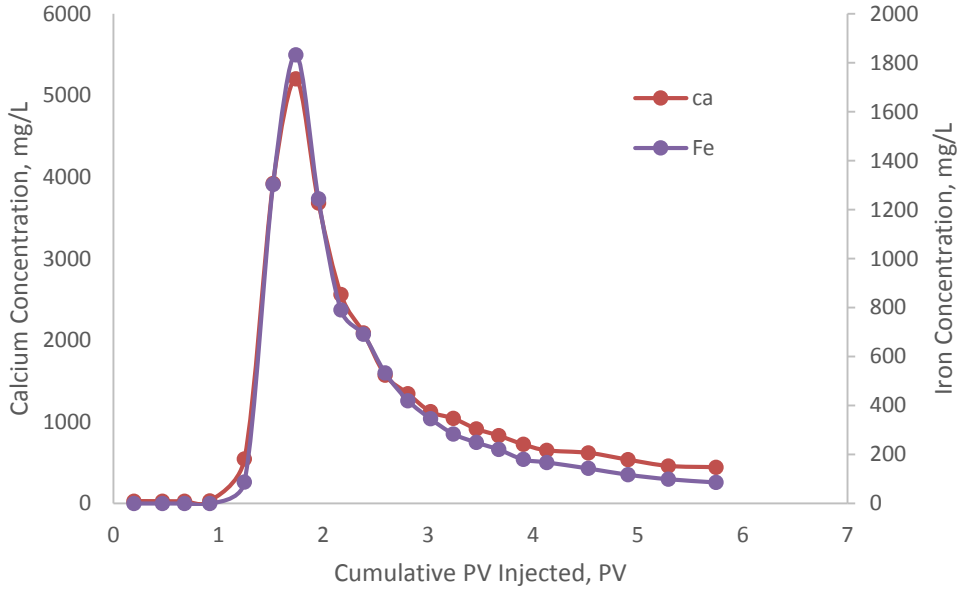

Fig. 18— Concentration of calcium and iron from limestone core, 5 wt% HCl 1vol% corrosion inhibitor and 10,000 ppm Fe(III) at 200 °F and 2 cm^3/min (Rady and Nasr-El-Din, 2015).

In the case of the Silurian dolomite, the initial permeability of the core was 121.8 md, and the final permeability was 103.1 md. After acidizing there was a 15.4% decrease in the permeability; this behavior was expected as a result of the iron injected into the formation. The damage in the case of the dolomite lithology was more severe than the damage in the limestone lithology. This is because the reaction between the hydrochloric acid and the $CaMg(CO_3)_2$ is slower compared to $CaCO_3$ due to the strong bond between the magnesium and oxygen. **Fig. 19** shows the pressure profile curve across the dolomite core. Following the acid injection, the pressure drop increased and stayed constant at the high value, indicating that the acid job damaged the formation. **Fig. 20** shows the inlet of the dolomite core after the injection of the acid. The figure further shows multiple small holes created as a result of the acid trying to create a path through the core. The core inlet is also covered in a reddish color which is the iron precipitant. The core effluent samples from the coreflood were analyzed using ICP. **Fig. 21** shows the concentration of the calcium, magnesium and iron in the effluent samples. Fig. 21 shows that the calcium and magnesium ions have the same trend; they both initially have a concentration of 0 mg/L and then reach a peak of 3,377 mg/l and 1,994 mg/l consecutively. Then, they gradually start to decrease. This is the same behavior that was observed in the Indiana limestone core, indicating that initially the collected sample is just DI water being displaced by the acid injected. The injected acid then reacts with the $CaMg(CO_3)_2$ to produce calcium and magnesium ions as byproducts. The gradual drop in the concentration of the calcium and magnesium ions is due to the dissociation of the hydrochloric acid. Fig. 21 also shows that the behavior of the iron concentration follows the same trend. Initially, no iron was

produced and then it started to gradually increase until it reached a maximum concentration of 2,755 mg/l and then it started to decrease again. In this core a total of 127.5 mg of iron was injected and 70.7 mg were produced in the effluent samples, which indicates that 55.5% of the iron was recovered. The pH of the samples was not measured because all the core effluent samples were diluted with hydrochloric acid to ensure that all iron was dissolved before ICP measurements were done. The damage in the dolomite core was nearly twice the damage in the limestone core. This means that having iron in the system greatly affects the acid job, and thus it is recommended to use iron-control agents in dolomite lithologies.

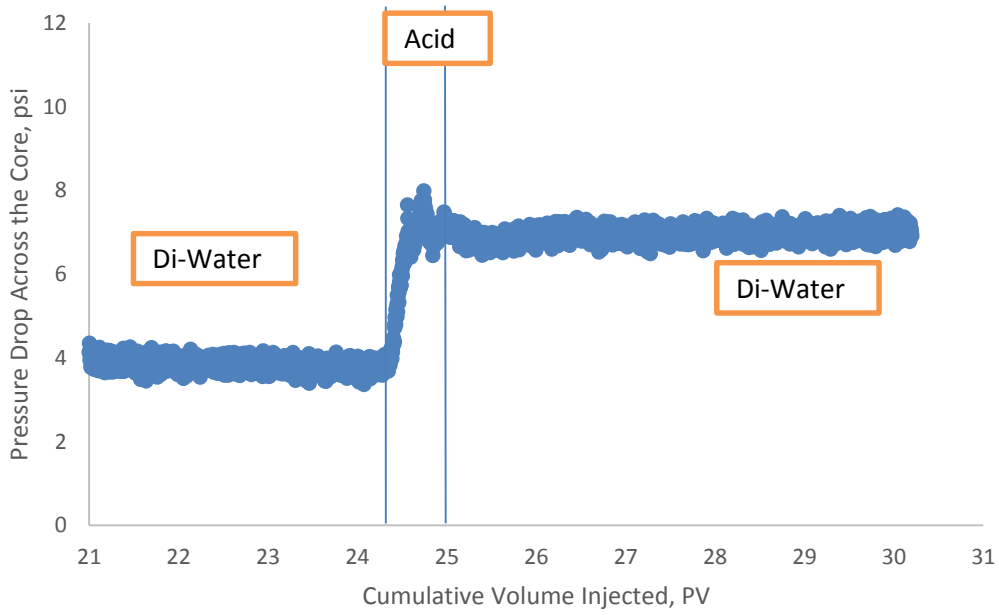

Fig. 19— Pressure profile across the dolomite core, 5 wt% HCl, 1 vol% corrosion inhibitor and 10,000 ppm Fe(III) at 200 °F and 2 cm^3/min (Rady and Nasr-El-Din, 2015).

Fig. 20— Dolomite core inlet after acidizing, 5 wt% HCl, 1 vol% corrosion inhibitor and 10,000 ppm Fe(III) at 200 °F and 2 cm^3/min (Rady and Nasr-El-Din, 2015).

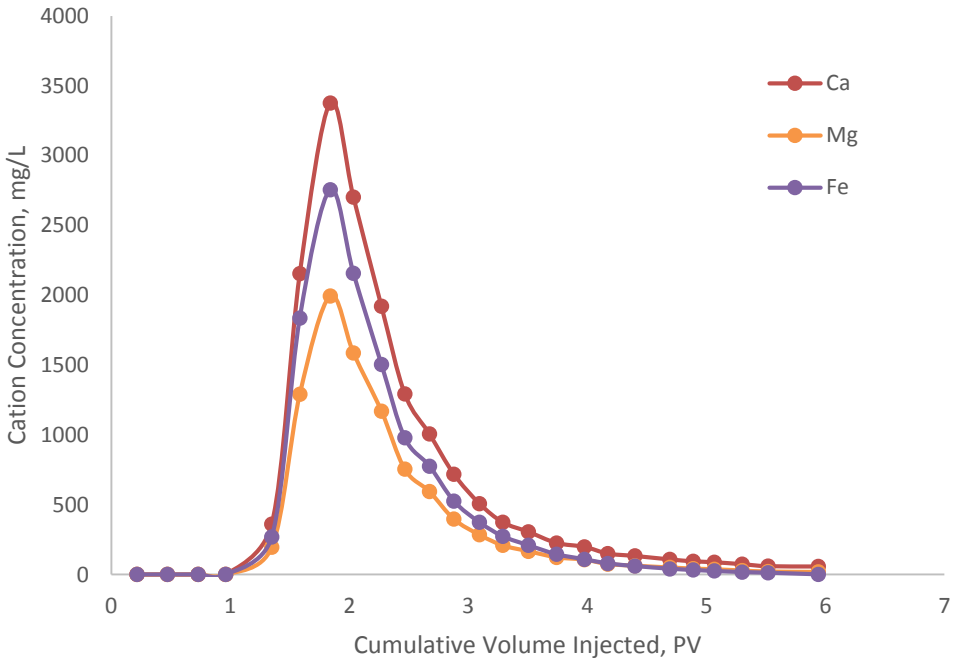

Fig. 21— Concentration of calcium, magnesium and iron from dolomite core, 5 wt% HCl, 1 vol% corrosion inhibitor and 10,000 ppm Fe(III) at 200 °F and 2 cm^3/min (Rady and Nasr-El-Din, 2015).

In the case of the Grey Berea sandstone the initial permeability of the core was 164 md and the final permeability was 139.6 md. After acidizing there was a 17% decrease in the permeability due to the precipitation on iron. **Fig. 22** shows the pressure profile curve across the sandstone core. The pressure drop was relatively constant during the entire experiment, even though the final permeability calculated shows damage. **Fig. 23** shows the inlet of the core after the injection of the acid, unlike the limestone and dolomite cores, there are no holes in the inlet of the core. The reddish color is also present in the sandstone core, indicating the damage due to the iron precipitation. The core effluent samples from the coreflood were analyzed using ICP. **Fig. 24** shows the concentration of the calcium and iron in the effluent samples. The behavior of the concentration of calcium followed the same trend as the limestone and dolomite formations; initially, the concentration of the calcium is 0 mg/l then it starts to increase until it reaches a peak of 3,771 mg/l, and then it drops again. The initial concentration of the iron produced back into the samples is 0 but then it starts to increase until it reaches a peak of 122,220 mg/l and then the concentration starts to drop back. In this core a total of 182 mg of iron is injected and 246 mg is recovered which is 135% of the original iron injected. The extra iron recovered can be attributed to the composition of the Grey Berea sandstone core. In this set of experiments the damage in the sandstone formation is greater than the damage in the limestone and dolomite formations. Once again the pH of the effluent samples was not measured, because they were diluted with hydrochloric acid to ensure that the iron is completely dissolved. However a study by Nasr-El-Din et al in 2002 studied the behavior of iron in mud acid. The study showed that Fe(III) precipitated at a pH of 0.6. Which means that the conditions

needed for Fe(III) to precipitate exist. It is evident that iron-control chemicals are needed when acidizing sandstone formations particularly as they contain iron compounds and the pH required for iron precipitation is 0.6 which is very low and definitely attained during acidizing.

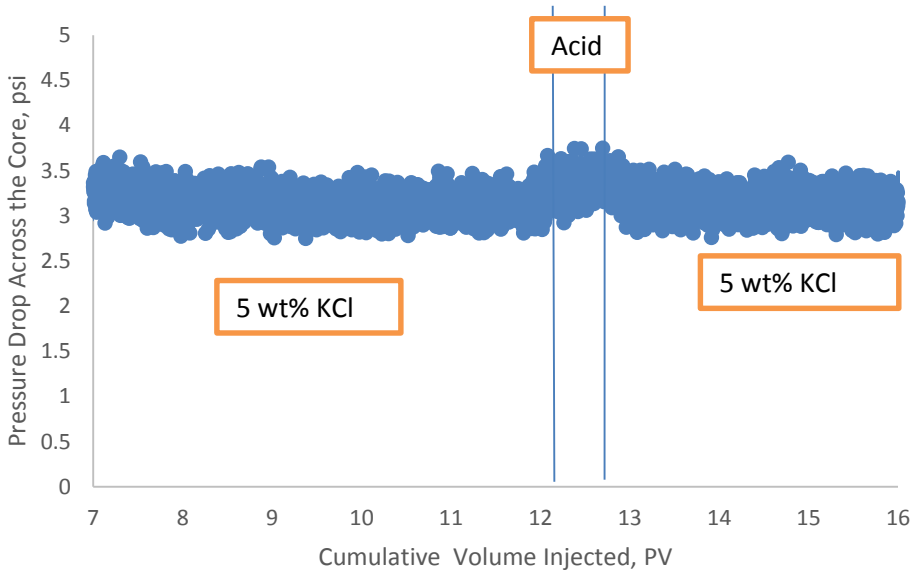

Fig. 22— Pressure profile across the sandstone core, 5wt% HCl, 1 vol% corrosion inhibitor and 10,000 ppm Fe(III) at 200 °F and 2 cm^3/min (Rady and Nasr-El-Din, 2015).

Fig. 23— Sandstone core inlet after acidizing, 5 wt% HCl, 1 vol% corrosion inhibitor and 10,000 ppm Fe(III) at 200 °F and 2 cm^3/min (Rady and Nasr-El-Din, 2015).

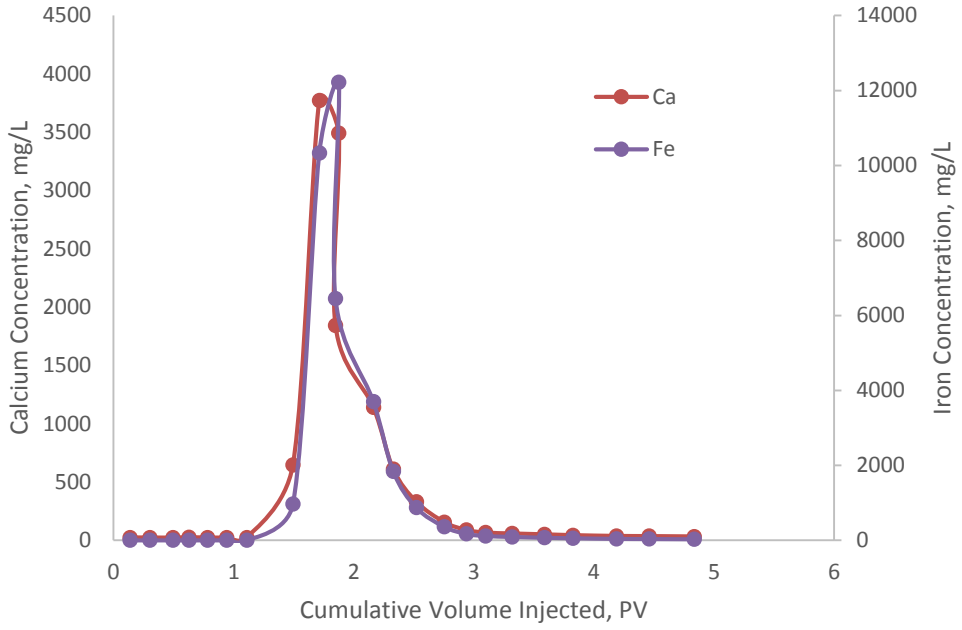

Fig. 24— Concentration of calcium and iron from the sandstone core, 5 wt% HCl 1 vol% corrosion inhibitor and 10,000 ppm Fe(III) at 200 °F and 2 cm^3/min (Rady and Nasr-El-Din, 2015).

Experimental Conditions 3

The third set of experiments involves the injection of 5 wt% hydrochloric acid, 2 wt% formic acid, 1 vol% corrosion inhibitor and 10,000 ppm of Fe(III) at 300 °F and a flowrate of 2 cm3/min. This set of experiments has the same exact conditions as the second set except for the temperature, which is set higher to study its effect on formation damage. Table 8 (Rady and Nasr-El-Din, 2015) summarizes the results from the experiments conducted.

Lithology	**Iron Recovered (%)**	**Initial Permeability (md)**	**Final Permeability (md)**	**Percent Change in Permeability**
Limestone	7.6	7.6	13.7	80.2% Increase
Dolomite	63	59.1	42.3	30% Decrease
Sandstone	70	218.6	86.2	60% Decrease

Table 8— Results of the coreflood experiment using 5 wt% HCl, 2 wt% CH_2O_2, 1 vol% corrosion inhibitor and 10,000 ppm Fe(III) at 300 °F and 2 cm^3/min (Rady and Nasr-El-Din, 2015).

The initial permeability of the Indiana limestone was 7.6 md and the final permeability was 13.7 md. The permeability of the limestone core increased by 80.2%. This increase was not expected because of the iron injected into the formation. **Fig. 25**

shows the pressure profile across the limestone core. During the acid injection, the pressure increased, but then it dropped and stabilized at a lower pressure. The increase in the pressure drop during the acid injection can be due to the increase in the viscosity of the injected fluid. The decrease in the pressure and the increase in the final permeability is due to the vigorous reaction between the acid and the calcium carbonate. The rate of the reaction between the acid and the limestone formation increases as the temperature increases, creating more channels and wormholes. As a result the iron did not cause formation damage in this case. The core effluent samples from the coreflood were analyzed using ICP, **Fig. 26** shows the concentration of the calcium and iron in the effluent samples. The concentration of the calcium ions also behaves in a similar fashion. The initial concentration of the calcium is 0 mg/l then it starts to increase until it reaches a peak of 14,260 mg/l, and then it drops again. The maximum concentration of calcium ions produced in this experiment is much higher than that produced in the previous cases. This high calcium concentration is due to the fast reaction rate that occurs as a result of the high temperature. Fig. 26 shows that iron was produced in the effluent samples. This result is expected as 120 mg of iron was injected in the system. The initial concentration of the iron produced back into the samples is 0 but then it starts to increase until it reaches a peak of 247 mg/l and then the concentration starts to drop back. The total iron recovered is 9.1 mg which is 7.6% of the original iron injected.

One explanation of the low percentage of iron recovered in the core effluent samples is that it can be due to the high concentration of calcium produced as a result of the vigorous reaction with HCl. The solubility of Fe (III) decreases with the increase in

divalent calcium cations. Moreover, at higher temperatures Fe(III) solubility decreases. Taylor el al. (1999b) showed that at 95 °C iron (III) hydroxide began to precipitate as the pH increased above 0.5. The results that are found in this thesis contradict those shown in a study by Assem et al (2013). That paper showed that by increasing the temperature from 200 °F to 300 °F, the percentage of iron recovered is greater. That study also showed that the permeability of the Indiana limestone core is better enhanced at 200 °F than at the higher temperature 300 °F (Assem el al. 2013).

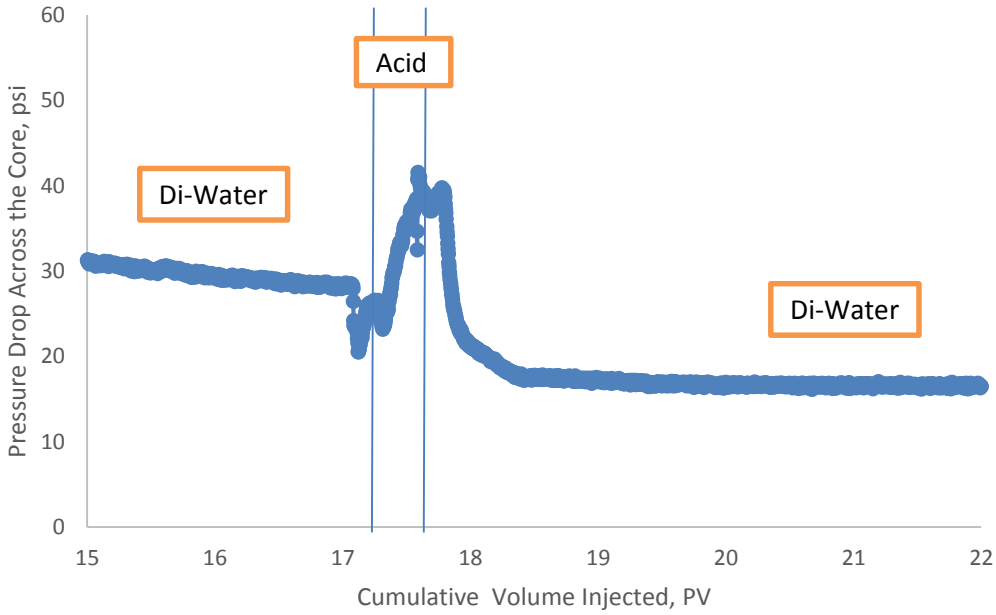

Fig. 25— Pressure profile across the limestone core, 5 wt% HCl, 1 vol% corrosion inhibitor, 2 wt% CH_2O_2 and 10,000 ppm Fe(III) at 300 °F and 2 cm^3/min (Rady and Nasr-El-Din, 2015).

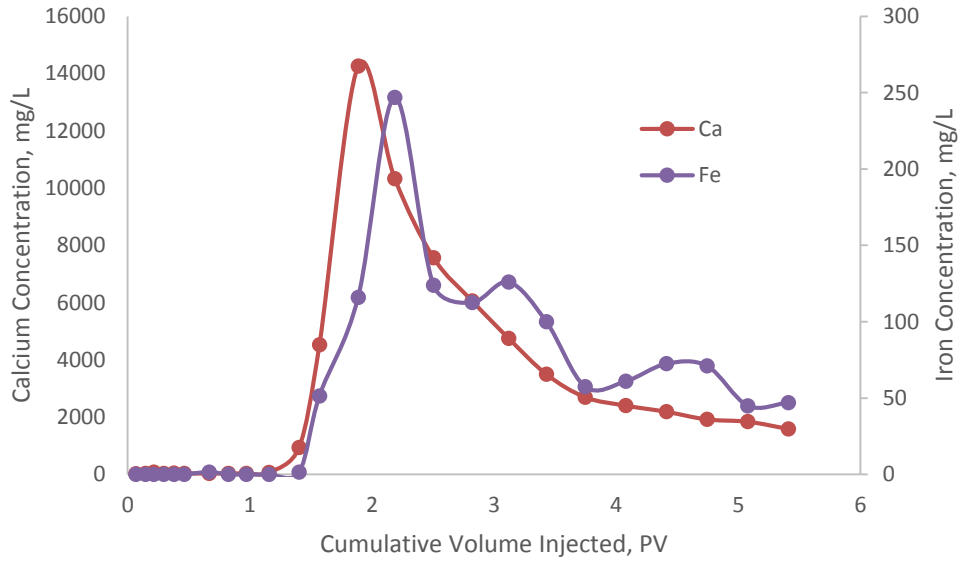

Fig. 26— Concentration of calcium and iron from limestone core, 5 wt% HCl, 1 vol% corrosion inhibitor, 2 wt % CH_2O_2, and 10,000 ppm Fe(III) at 300 °F and 2 cm^3/min (Rady and Nasr-El-Din, 2015).

In the case of the Silurian dolomite, the initial permeability of the core was 59.1 md and the final permeability was 42.3 md. After acidizing there was a 30% decrease in the permeability; this behavior is a result of the iron injected into the formation. Unlike the limestone formation, the dolomite was damaged. This is because the reaction between the hydrochloric acid and the $CaMg(CO_3)_2$ is slower compared to $CaCO_3$ as explained earlier. **Fig. 27** shows the pressure profile curve across the dolomite core. Following the acid injection, the pressure drop increased and stayed constant at the higher value indicating that the acid job damaged the formation. The core effluent samples from the coreflood were analyzed using ICP. **Fig. 28** shows the concentration of the calcium, magnesium and iron in the effluent samples. Fig. 28 shows that the calcium and magnesium ions have the same trend; they both initially have a

concentration of 0 mg/l and then reach a peak of 7,630 mg/l and 4,922 mg/l consecutively, then they gradually start to decrease. The concentration of the calcium and magnesium produced in this case is much higher than in the previous case even though the same acid and iron concentrations are used. This increase is due to the increase in the temperature, causing a slightly faster reaction between the acid and the $CaMg(CO_3)_2$. The behavior of the iron concentration follows the same trend. Initially, no iron was produced, but then it started to gradually increase till it reached a maximum concentration of 3,428 mg/l and then it started to decrease again. In this core a total of 119.4 mg of iron was injected and 75.3 mg were produced in the effluent samples which indicates that 63% of the iron was recovered. Increasing the temperature did not enhance the core final permeability as in the case of the Indiana limestone core. On the contrary, the damage was more intense at the high temperature conditions. Once again it is recommended to use iron-control agents when acidizing a dolomite formation.

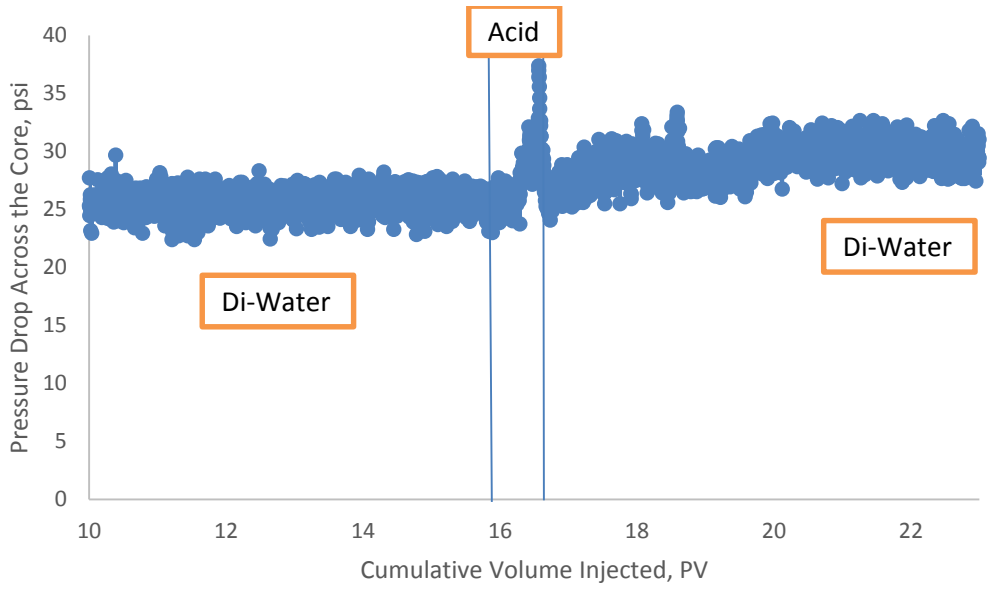

Fig. 27— Pressure profile across the dolomite core, 5 wt% HCl, 1 vol% corrosion inhibitor, 2 wt% CH_2O_2 and 10,000 ppm Fe(III) at 300 °F and 2 cm^3/min (Rady and Nasr-El-Din, 2015).

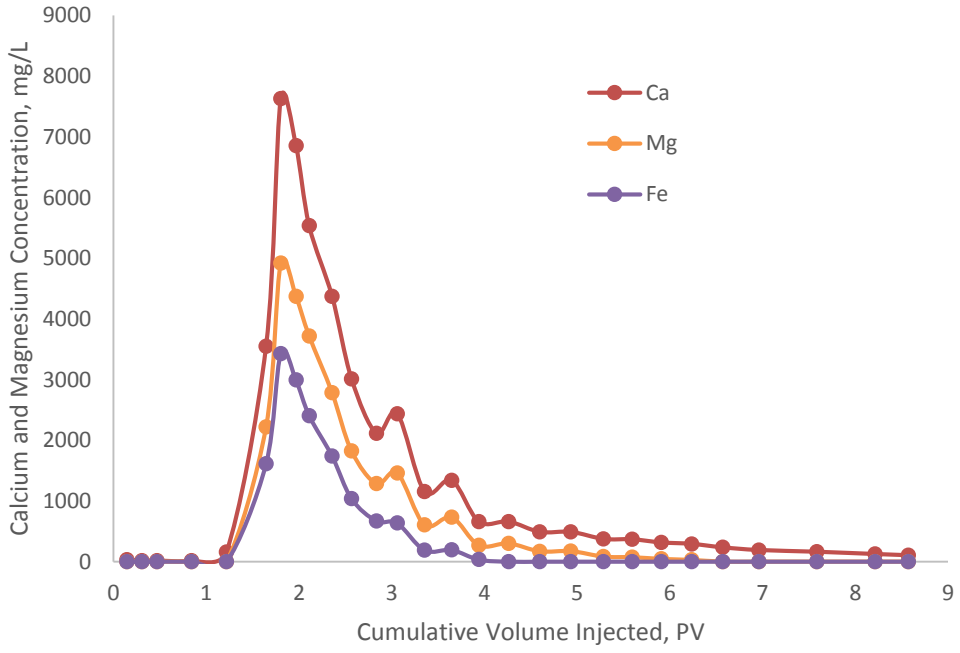

Fig. 28— Concentrations of calcium, magnesium, and iron from the dolomite core, 5 wt% HCl, 1 vol% corrosion inhibitor, 2 wt% CH_2O_2 and 10,000 ppm Fe(III) at 300 °F and 2 cm^3/min (Rady and Nasr-El-Din, 2015).

In the case of the Grey Berea sandstone the initial permeability of the core was 218.6 md and the final permeability was 86.2 md. After acidizing, there was a 60% decrease in the permeability. **Fig. 29** shows the pressure profile curve across the sandstone core. Once again, the pressure drop is relatively constant during the entire experiment, even though the final permeability calculated shows damage. The core effluent samples from the coreflood were analyzed using ICP. **Fig. 30** shows the concentration of the calcium and iron in the effluent samples. Initially the concentration of the calcium is 0 mg/l, then it starts to increase till it reaches a peak of 40.5 mg/l, and then it drops again and finally increases once more. The initial concentration of the iron produced back in the samples is 0, but then it starts to increase until it reaches a peak of 9,575 mg/l and then the concentration starts to drop back. In this core, a total of 157.5 mg of iron was injected and 110.9 mg was recovered, which is 70.4 % of the original iron injected. Similar to the case of the Indiana limestone core, the low percentage of iron recovered in the core effluent samples can be due to the high concentration of calcium produced. The maximum concentration of calcium produced in this case in 9,575 mg/l while at 200 °F, the maximum calcium concentration produced was 3,771 mg/l. Moreover, the solubility of Fe(III) decreases at higher temperatures as mentioned earlier. Another factor to consider is the clay particles stability at high temperature. The study by Musharova el al. (2012) conducted coreflood experiments on Grey Berea sandstone cores and found that the clay particle stability is affected by temperature. At high temperatures, the migration process of the clays becomes faster because the clay fines become sensitive and detach from the rock surface. This means that at high temperatures the damage in sandstone formations

will be much more severe because of the multiple parameters discussed. Once again, in this set of experiments, the damage in the sandstone lithology is much greater than that seen in dolomite. This finding shows that iron-control chemicals are definitely needed in sandstone formations.

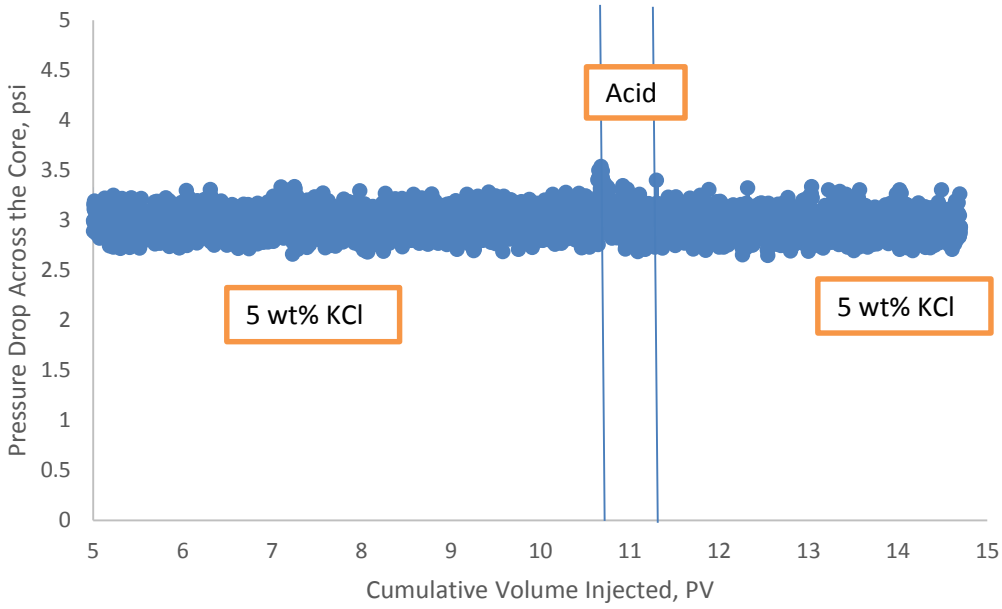

Fig. 29— Pressure profile across the sandstone core, 5 wt% HCl, 1 vol% corrosion inhibitor, 2 wt% CH_2O_2 and 10,000 ppm Fe(III) at 300 °F and 2 cm^3/min (Rady and Nasr-El-Din, 2015).

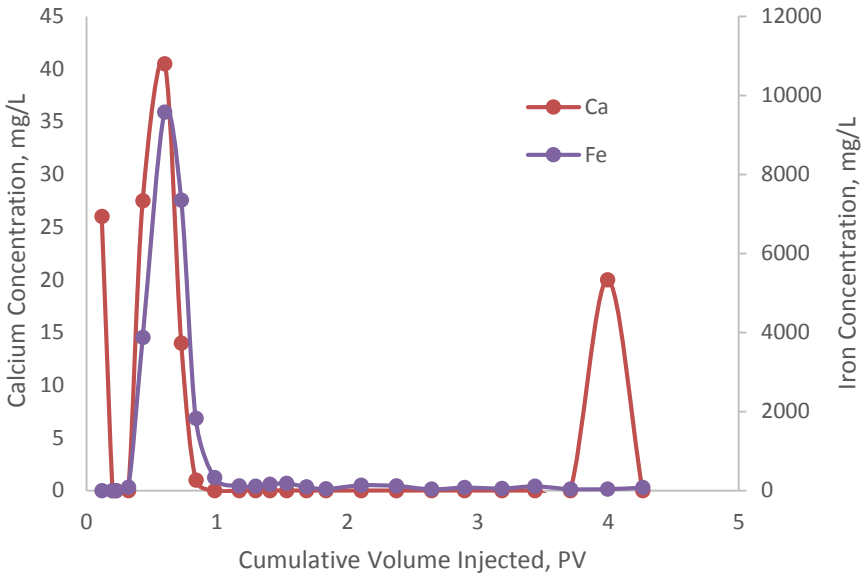

Fig. 30— Concentration of calcium and iron from sandstone core, 5 wt% HCl, 1 vol% corrosion inhibitor, 2 wt % CH_2O_2 and 10,000 ppm Fe(III) at 300 °F and 2 cm^3/min (Rady and Nasr-El-Din, 2015).

Experimental Conditions 4

The fourth set of experiments involved the injection of 5 wt% hydrochloric acid, 1 vol% corrosion inhibitor and 5,000 ppm of Fe(III) at 200 °F and a flowrate of 2 cm^3/min. This set of experiments aims at studying the effect of the iron concentration on the damage that occurs in the three lithologies. **Table 9** (Rady and Nasr-El-Din, 2015) summarizes the results from the experiments conducted.

Lithology	Iron Recovered (%)	Initial Permeability (md)	Final Permeability (md)	Percent Change in Permeability
Limestone	35.8	67	115	67% Increase
Dolomite	46	140	140	No change
Sandstone	410	155.4	150.9	2.8% Decrease

Table 9— Results of the coreflood experiment using 5 wt% HCl, 1 vol% corrosion inhibitor and 5,000 ppm Fe(III) at 200 °F and 2cm^3/min (Rady and Nasr-El-Din, 2015).

The initial permeability of the Indiana limestone was 67 md and the final permeability was 115 md. The permeability of the limestone core increase by 67%. **Fig. 31** shows the pressure profile across the limestone core. During the acid injection, the pressure dropped and stabilized at a lower pressure, indicating a successful acid treatment. Decreasing the iron concentration to 5,000 ppm did not have an adverse effect on the limestone core. The results presented here follow the same results presented in the study by Assem et al. 2013. Decreasing the concentration of iron causes less damage to the Indiana limestone core. Moreover, having an iron concentration of 5,000 ppm does not cause any damage to the core; on the contrary, there was a 67% increase in the final permeability after acidizing. The study by Assem et al. showed only a 12% increase in the final permeability of core after acidizing with the same conditions. The core effluent samples from the coreflood were analyzed using ICP, **Fig. 32** shows the concentration of the calcium and iron in the effluent samples. Fig. 32 shows that iron was produced in the

effluent samples, and this is expected as 61.7 mg of iron was injected in the system. The initial concentration of the iron produced back in the samples is 0, then it starts to increase until it reaches a peak of 247 mg/l and then the concentration starts to drop back. The total iron recovered is 9.1 mg, which is 7.6% of the original iron injected. The concentration of the calcium ions also behaves in a similar fashion. The initial concentration of the iron is 0 mg/l then it starts to increase until it reaches a peak of 748.1 mg/l and then it drops again. The calcium concentration initially is 0, then it starts to increase till it reaches a peak value of 4,490 mg/l, then it drops again. From this experiment, it can be agreed that there is a certain limit for the iron concentration that does not affect the acid job. The results presented indicate that there is a certain limit to which iron precipitation in the Indiana limestone formation does not adversely affect the permeability of the core. In this case, it is evident that iron-control chemicals are not needed.

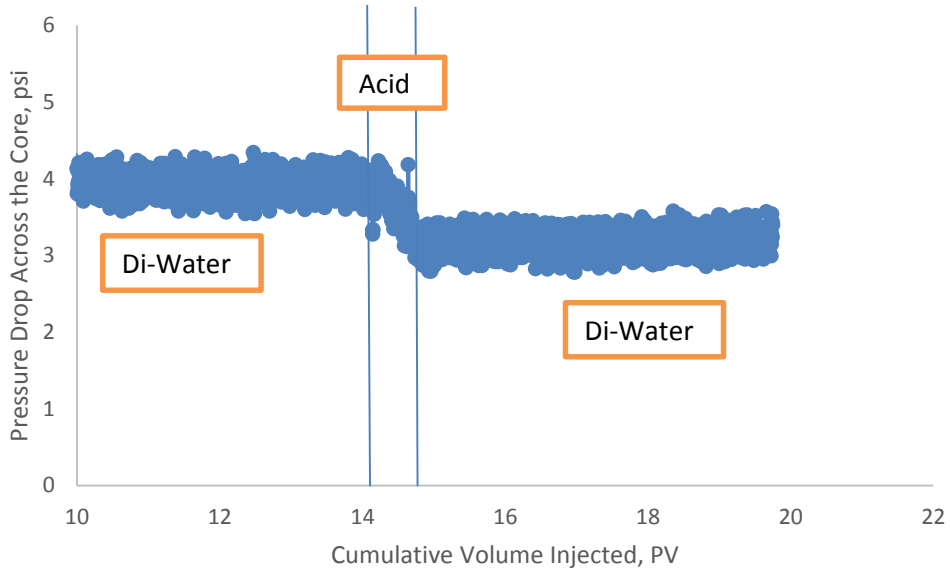

Fig. 31— Pressure profile across the limestone core, 5 wt% HCl, 1 vol% corrosion inhibitor and 5,000 ppm Fe(III) at 200 °F and 2 cm^3/min (Rady and Nasr-El-Din, 2015).

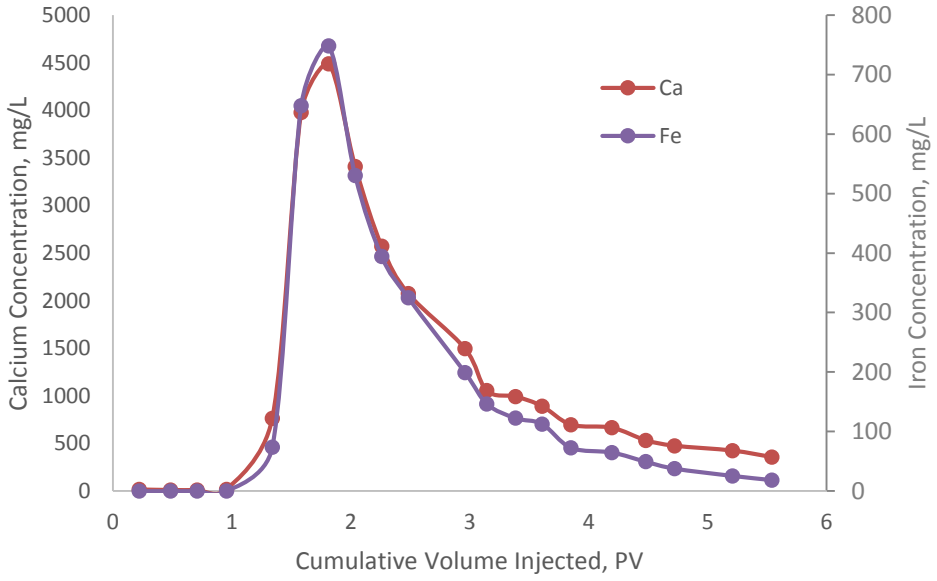

Fig. 32— Concentration of calcium and iron from the limestone core, 5 wt% HCl, 1 vol% corrosion inhibitor and 5,000 ppm Fe(III) at 200 °F and 2 cm^3/min (Rady and Nasr-El-Din, 2015).

The initial permeability of the Silurian dolomite core was 140 md and the final permeability was 140 md. The permeability of the dolomite core wasn't affected by acidizing. **Fig. 33** shows the pressure profile across the dolomite core. The pressure remained relatively constant during the entire experiment. Decreasing the iron concentration to 5,000 ppm did not cause damage, but at the same time did not enhance the permeability. The core effluent samples from the coreflood were analyzed using ICP, **Fig. 34** shows the concentration of the calcium, magnesium and iron in the effluent samples. Fig. 34 further shows the usual behavior of the calcium and magnesium concentrations starting at 0 and increasing to reach a peak of 3,352 mg/l and 2,012 mg/l respectively, then dropping back. The initial concentration of the iron produced back in to the samples is 0, then it starts to increase until it reaches a peak of 1,139 mg/l and then the concentration starts to drop back. The total iron injected into this dolomite core was 62.75 mg of which 28.89 mg were recovered, or is 40% of the original iron injected. Decreasing the iron concentration to 5,000 ppm resulted in a failed acid job as the permeability of the core remained unchanged. This shows that the dolomite formation is very sensitive to any precipitation. Iron-control chemicals should be used in dolomite formations because any precipitation will lead to a failed job and a waste of resources.

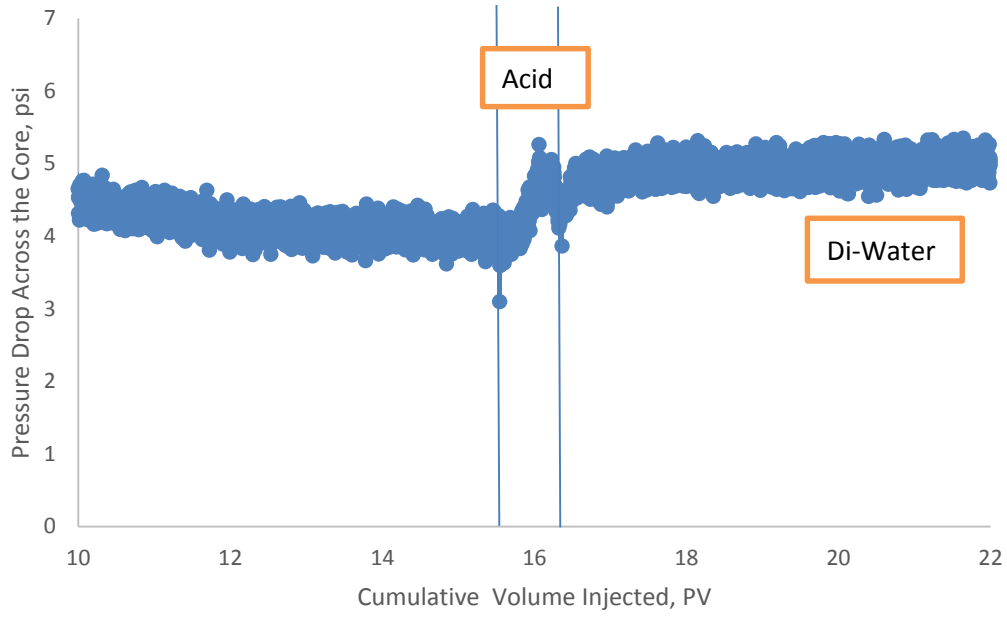

Fig. 33— Pressure profile across the dolomite core, 5 wt% HCl, 1 vol% corrosion inhibitor and 5,000 ppm Fe(III) at 200 °F and 2 cm^3/min (Rady and Nasr-El-Din, 2015).

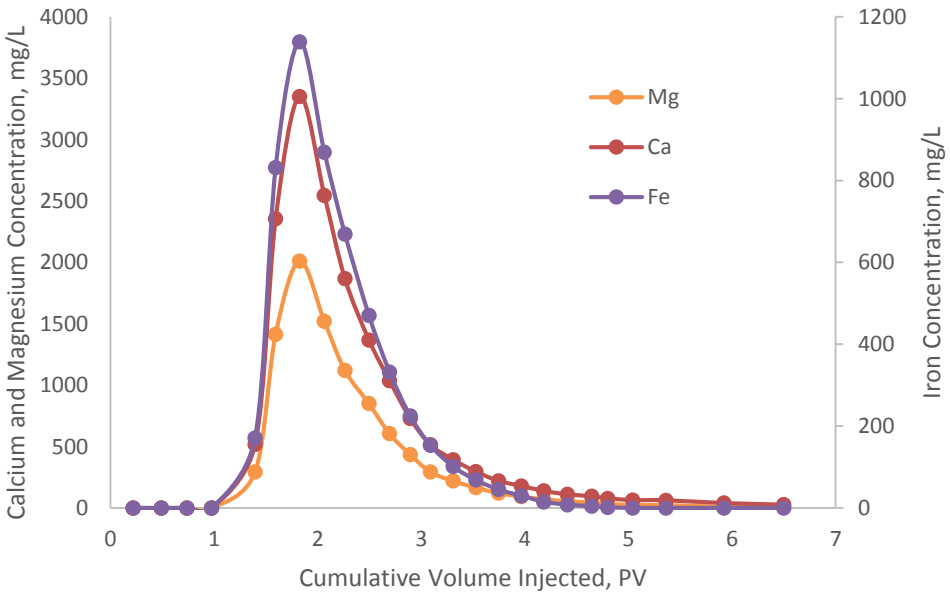

Fig. 34— Concentration of calcium, magnesium and iron from dolomite core, 5 wt% HCl, 1 vol% corrosion inhibitor and 5,000 ppm Fe(III) at 200 °F and 2 cm^3/min (Rady and Nasr-El-Din, 2015).

The initial permeability of the Grey Berea sandstone core was 155.4 md and the final permeability was 150.9 md. The permeability of the sandstone core decreased by 2.8% after the acid injection. **Fig. 35** shows the pressure profile across the sandstone core. The pressure remained relatively constant during the entire experiment. Decreasing the iron concentration to 5,000 ppm did not cause as much damage as was shown when the iron concentration to 5,000 ppm did not cause as much damage as was shown when the concentration was 10,000 ppm. The core effluent samples from the coreflood were analyzed using ICP. **Fig. 36** shows the concentration of the calcium and iron in the effluent samples. Fig. 36 further shows the usual behavior of the calcium and iron concentrations starting at 0 and increasing to reach a peak of 6,982 mg/l and 13,900 mg/l respectively, then dropping back. The total iron injected into this sandstone core was 86.4 mg and 354.5 mg were recovered, which is 410% of the original iron injected. In all the sandstone cases presented in this study, there was always a decrease in the permeability, and, hence, formation damage. The damage increased as there was more iron in the system. Decreasing the concentration of iron from 10,000 ppm to 5,000 ppm caused the percentage of permeability decrease to go from 17% to 2.8%. This shows how iron in the system has detrimental effects on the sandstone formations in particular. It can be concluded that iron-control agents are especially needed when acidizing sandstone formations.

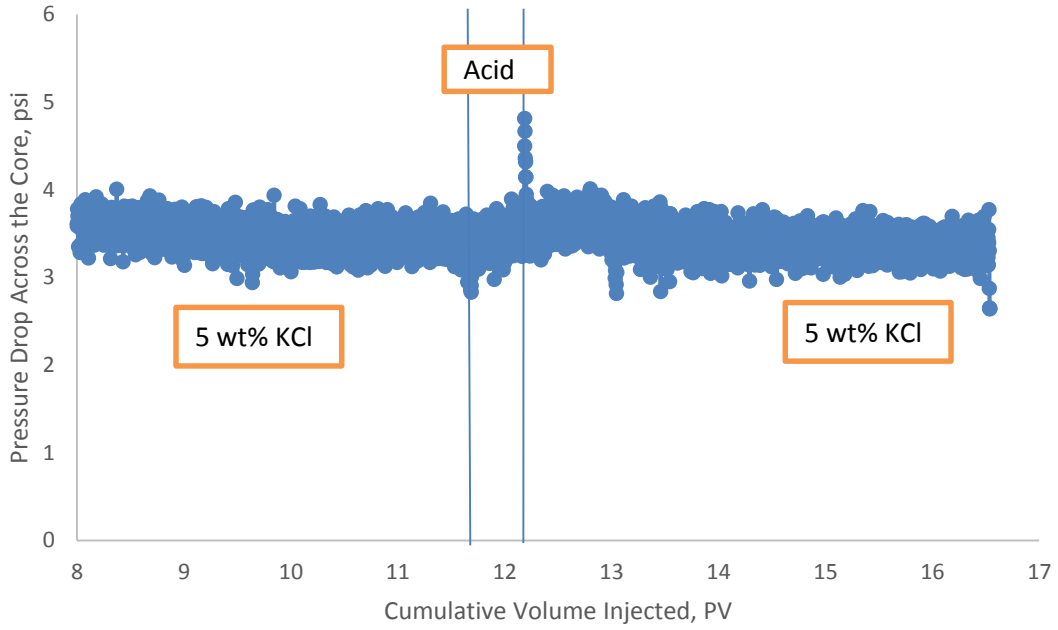

Fig. 35— Pressure profile across the sandstone core, 5 wt% HCl, 1 vol% corrosion inhibitor and 5,000 ppm Fe(III) at 200 °F and 2 cm^3/min (Rady and Nasr-El-Din, 2015).

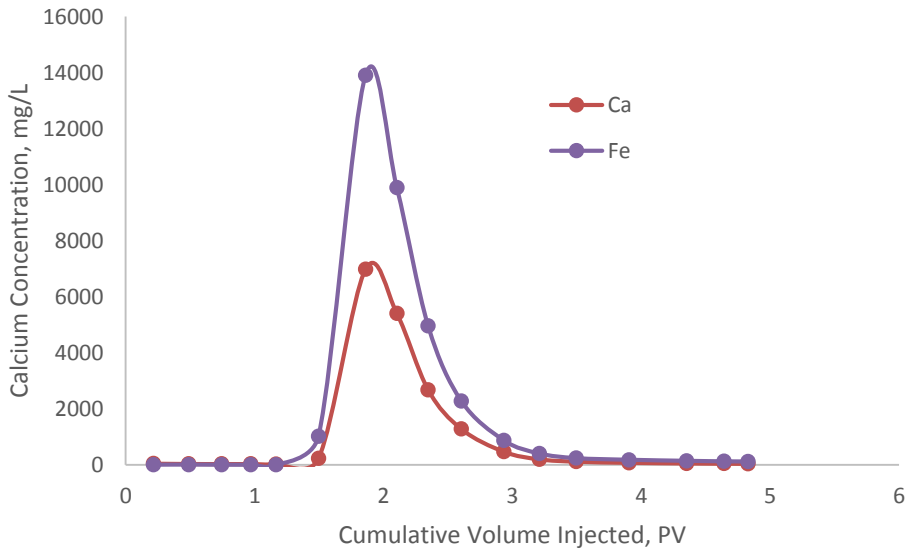

Fig. 36— Concentration of calcium and iron from sandstone core, 5 wt% HCl, 1 vol% corrosion inhibitor and 5,000 ppm Fe(III) at 200 °F and 2 cm^3/min (Rady and Nasr-El-Din, 2015).

CHAPTER IV

CONCLUSIONS AND RECOMMENDATIONS

Formation damage due to iron precipitation is a critical problem faced during acid well stimulation. The presence of iron can cause the acid job to fail and can result in more damage than the original state of the well prior to acidizing. Hence, it is very important to reduce the amount of iron that can enter the formation during acidizing; this can be done by pickling the tubings, mixing tanks, storage tanks, and lines before acid injection. This research compared three different lithologies to examine the effect of iron precipitation. Temperature and iron concentration where varied to understand the effect of iron precipitation in the three different lithologies. The following conclusions were made:

- Limestone formation are the least affected by iron precipitation
- The permeability of the limestone formations was enhanced in all the cases except one
- Iron control agents should be used to get better enhancement in limestone formations
- In the case of dolomite iron resulted in formation damage in all the conditions tested
- In dolomite more damage occurred at high temperatures
- Iron control agents are necessary when acidizing dolomite formations
- Iron precipitation is more complicated in sandstone formations due to the iron and clay content in the core

- Damage was evident in all the cases in the sandstone cores
- At higher temperature more damage occurs due to fines migration in sandstone formations
- Iron control agents are needed along with clay stabilizers in sandstone cores

REFERENCES

Alkattan, M., Oelkers, E.H., Dandurand, J.L., Schott, J. 1998. An Experimental Study of Calcite and Limestone Dissolution Rates as a Function of pH from −1 to 3 and Temperature from 25 to 80°C. Chemical Geology Journal **151** (1-4): 199-214, doi.org/10.1016/S0009-2541(98)00080-1.

Anderson, M. S. 1991. Reactivity of San Andres Dolomite. SPE Prod & Engineering **6** (2): 227-232. doi:10.2118/20115-PA.

Assem, A.I., Nasr-El-Din, H.A., and De Wolf, C.A. 2013. Formation Damage Due To Iron Precipitation in Carbonate Rocks. Paper presented at the SPE European Formation Damage Conference and Exhibition, Noordwijk, The Netherlands, 5-7 June. SPE 165203-MS. http://doi:10.2118/165203-MS.

Assem, A.I. Formation Damage Due to Iron Precipitation During Matrix Acidizing Treatments of Carbonate Reservoirs and Ways to Minimize it Using Chelating Agents. 2013.

Crowe, C.W. 1986. Prevention of Undesirable Precipitates from Acid Treating Fluids. Paper presented at the International Meeting on Petroleum Engineering, Beijing, China, 17-20 March. SPE 14090-MS. http://doi:10.2118/14090-MS.

Dill, W.R. and Fredette, G. 1983. Iron Control in the Appalachian Basin. Paper presented at the SPE Eastern Regional Meeting, Pittsburgh, Pennsylvania, 9-11 November. SPE 12319-MS. http://doi:10.2118/12319-MS.

Dill, W. and Smolarchuk, P. 1988. Iron Control In Fracturing and Acidizing Operations Journal of Petroleum Technology **23** (03): 75-78. PETSOC-88-03-08. http://doi:10.2118/88-03-08.

Garzon, F.O., Nasr-El-Din, H.A., Al-Mutairi, S.H., et al. 2007. Lessons Learned from Re-Pickling Old/Sour Gas Wells. Paper presented at the SPE Middle East Oil and Gas Show and Conference, Manama, Bahrain, 11-14 March. SPE 105633-MS. http://doi:10.2118/105633-MS.

Ghommem, M., Zhao W., Dyer, S., Qiu, X., Brady, D. 2015. Carbonate acidizing: Modeling, Analysis, and Characterization of Wormhole Formation and Propagation. Journal of Petroleum Science and Engineering **131**:18-33. dx.doi.org/10.1016/j.petrol.2015.04.021.

Gougler, P.D., Hendrick, J.E., and Coulter, A.W. 1985. Field Investigation Identifies Source and Magnitude of Iron Problems. Paper presented at the SPE Production Operations Symposium, Oklahoma City, Oklahoma, 10-12 March. SPE 13812-MS. http://doi:10.2118/13812-MS.

Hanafy, A., Ali, A., Nasr-El-Din, H. A., & Heidari, Z. 2015. Evaluating the Effects of Acid Stimulation Treatment Before and After Fines Migration on Petrophysical Properties in Sandstone Reservoirs. Paper presented at SPE International Petroleum Technology Conference 6-9 December, Doha, Qatar. doi:10.2523/IPTC-18569-MS.

Hoefner, M. L. and Fogler, H. S. 1988. Pore Evolution and Channel Formation During Flow and Reaction in Porous Media. American Institute of Chemical Engineers Journal **34**: 45–54. doi:10.1002/aic.690340107.

Ji, Q., Zhou, L., & Nasr-El-Din, H. 2015. Acidizing Sandstone Reservoirs with Aluminum-Based Retarded Mud Acid. SPE Journal Preprint. doi:10.2118/169395-PA.

Kia, S. F., Fogler, H. S., Reed, M. G., & Vaidya, R. N. 1987. Effect of Salt Composition on Clay Release in Berea Sandstones. SPE Prod Engineering **2** (04): 277-283 . doi:10.2118/15318-PA.

Khilar, K. C., & Fogler, H. S. 1983. Water Sensitivity of Sandstones. SPE Journal **01** (23): 55-64. doi:10.2118/10103-PA.

Lund, K. Fogler, H.S., McCune, C.C. 1973. Acidization—I The dissolution of Dolomite in Hydrochloric Acid. Chemical Engineering Science Journal **28** (3): 691-700 dx.doi.org/10.1016/0009-2509(77)80003-1.

Musharova, D., Mohamed, I. M., & Nasr-El-Din, H. A. 2012. Detrimental Effect of Temperature on Fines Migration in Sandstone Formations. Paper presented at SPE International Symposium and Exhibition on Formation Damage Control, 15-17 February, Lafayette, Louisiana, USA. doi:10.2118/150953-MS.

Nasr-El-Din, H. A., Al-Dahlan, M. N., As-Sadlan, A. M., & Al-Zamil, H. A. 2002. Iron Precipitation during Acid Treatments Using HF-Based Acids. Paper presented at SPE International Symposium and Exhibition on Formation Damage Control, 20-21 February, Lafayette, Louisiana. doi:10.2118/73747-MS.

Nasr-El-Din, H. A., Al-Mohammed, A. M., Al-Aamri, A., & Al-Fuwaires, O. A. 2008. Reaction of Gelled Acids with Calcite. SPE Production and Operations **23** (03): 353-361. doi:10.2118/103979-PA

Rabie, A.I. and Nasr-El-Din, H.A. 2015. Sodium Gluconate as a New Environmentally Friendly Iron Controlling Agent for HP/HT Acidizing Treatments. Paper presented at the SPE Middle East Oil & Gas Show and Conference, Manama, Bahrain, 8-11 March. SPE 172640-MS. http://doi:10.2118/172640-MS.

Rady, A., and Nasr-El-Din, H. A. 2015. Iron Precipitation in Calcite, Dolomite and Sandstone Cores. Paper presented at SPE Russian Petroleum Technology Conference, 26-28 October, Moscow, Russia. doi:10.2118/176574-MS

Sayed, M., Nasr-El-Din, H. A., & Nasrabadi, H. 2013. Reaction of Emulsified Acids with Dolomite. Journal of Canadian Petroleum Technology **52** (03): 164-175. doi:10.2118/151815-PA.

Schembre, J. M., & Kovscek, A. R. 2004. Thermally Induced Fines Mobilization: Its Relationship to Wettability and Formation Damage. Paper presented at SPE International Thermal Operations and Heavy Oil Symposium and Western Regional Meeting, 16-18 March, Bakersfield, California. doi:10.2118/86937-MS

Smith, C.F., Crowe, C.W., and Nolan, T.J. 1969. Secondary Deposition of Iron Compounds Following Acidizing Treatments. SPE Journal of Petroleum Technology **21** (9): 1121-1129. SPE 2358-PA. http://doi:10.2118/2358-PA.

Taylor, K. C., Al-Ghamdi, A. H., & Nasr-El-Din, H. A. 2004. Measurement of Acid Reaction Rates of a Deep Dolomitic Gas Reservoir. Journal of Canadian Petroleum Technology **10** (43): 49-56. doi:10.2118/04-10-05.

Taylor, K.C. and Nasr-El-Din, H.A. 1999. A Systematic Study of Iron Control Chemicals Part 2. Presented at the SPE International Symposium on Oilfield Chemistry, Houston, Texas, 16-19 February. SPE 50772-MS. http://doi:10.2118/50772-MS.

Taylor, K. C., Nasr-El-Din, H. A., & Saleem, J. A. 2001. Laboratory Evaluation of Iron-Control Chemicals for High-Temperature Sour-Gas Wells. Paper presented at SPE International Symposium on Oilfield Chemistry, 13-16 February, Houston, Texas. doi:10.2118/65010-MS.

Taylor, K. C., Nasr-El-Din, H. A., & Mehta, S. 2006. Anomalous Acid Reaction Rates in Carbonate Reservoir Rocks. SPE Journal **4** (11): 488-496. doi:10.2118/89417-PA.

Tchistiakov, A. A. 2000. Colloid Chemistry of In-Situ Clay-Induced Formation Damage. Paper presented at SPE International Symposium on Formation Damage Control, 23-24 February, Lafayette, Louisiana. doi:10.2118/58747-MS.

Walker, M.L., Dill, W.R., Besler, M.R. et al. 1991. Iron Control in West Texas Sour-Gas Wells Provides Sustained Production Increases. SPE Journal of Petroleum Technology **43** (5): 603-607. SPE 20122-PA. http://doi:10.2118/20122-PA.